Protection against high fat diet induced obesity in *mdx* mice: is sarcolipin involved?

by

Frenk Kwon

A thesis
presented to the University of Waterloo
in fulfillment of the
thesis requirement for the degree of
Master of Science
in
Kinesiology

Waterloo, Ontario, Canada, 2018
© Frenk Kwon 2018

AUTHOR'S DECLARATION

I hereby declare that I am the sole author of this thesis. This is a true copy of the thesis, including any required final reversions, as accepted by my examiners.

I understand that my thesis may be made electronically available to the public.

Abstract

Sarcolipin (SLN) is a 31 amino acid proteolipid and one of the regulators of sarco(endo)plasmic reticulum Ca^{2+}-ATPase (SERCA) pumps. Previous research has shown that sarcolipin levels in muscles from wild type (WT) mice increase 2-3 fold in response to consuming a high fat diet, possibly to help mitigate obesity by increasing energy expenditure and burning excess calories. The role of SLN in diet-induced thermogenesis was shown in subsequent studies via high fat feeding of *Sln*-null mice. In response to consuming a high-fat diet (HFD), *Sln*-null animals have significantly greater mass and adiposity, in addition to poorer glucose handling, compared with WT mice. Higher than normal levels of SLN have also been found in *mdx* mice, a murine model of Duchenne muscular dystrophy. Interestingly, it was reported that *mdx* mice are protected from obesity after high fat feeding. The purpose of this thesis was two-fold: (1) to determine if *mdx* mice fed a Westernized diet are protected from diet-induced obesity, and (2) to determine the role of SLN in protecting *mdx* mice against diet-induced obesity. WT, mdx, and *mdx/Sln*-null mice consumed a Westernized high-fat diet (42% kcal from fat) for 8 weeks while measurements of body weight and food consumption were made on a weekly basis. Glucose tolerance testing (GTT) and measurements of whole body daily metabolic rate with the comprehensive laboratory animal monitoring system (CLAMS) were performed before and after the diet protocols. Western blotting was conducted to determine the relative expression levels of SLN in diaphragm (DIA) and uncoupling protein (UCP)-1 in brown adipose tissue (BAT) from all animals. Fat pads were collected to calculate relative adiposity to determine the level of obesity in all animals. As expected, in response to the high-fat diet, *mdx* but not *mdx/Sln*-null mice gained less weight and adiposity ($P < 0.05$) in comparison to WT mice. Compared with *mdx* mice, *mdx/Sln*-null mice did not gain more weight but were more obese ($P < 0.05$) following the high-fat diet. Whole body metabolic rate (ml O_2/kg/hr) was higher ($P < 0.05$) in *mdx* mice in comparison

to WT and *mdx/Sln*-null mice before and after the high-fat diet, which may explain the lower diet-induced obesity in *mdx* mice. With increased obesity, *mdx/Sln*-null mice became extremely ($P<0.05$) glucose intolerant, more so than WT and *mdx* mice. Interestingly, *mdx* mice saw no change in glucose tolerance when compared with pre-HFD values, suggesting that *mdx* mice were protected from HFD-induced glucose intolerance. Western blotting analyses revealed SLN content was 2-fold higher in chow-fed *mdx* mice compared to chow-fed WT mice. Although SLN expression in DIA remained higher in *mdx* compared with WT post-HFD, it decreased in response to the high-fat diet in *mdx* mice and was unchanged in WT mice. UCP-1 expression was found to be higher ($P<0.05$) after the high-fat diet in all three genotypes, but there were no significant genotype differences in UCP-1 expression despite *mdx/Sln*-null mice having greater BAT weights compared with *mdx* mice. Altogether, these results suggest that SLN could play a role in adaptive diet-induced thermogenesis in *mdx* mice and provide protection against diet-induced obesity and glucose intolerance. However, despite the higher ($P<0.05$) daily VO_2 in *mdx* compared to *mdx/Sln*-null mice post-HFD, both saw a non-significant differences in absolute sleeping VO_2 comparison to pre-diet values. Thus, it is possible that other thermogenic mechanisms may have caused the increase in resting VO_2 of *mdx/Sln*-null mice.

Acknowledgements

First and foremost, I must sincerely thank my supervisor, Dr. A. Russell Tupling, for giving me an opportunity to be part of such a wonderful laboratory. Your support and patience the last three years, through all the complications and tribulations has been greatly appreciated. Your support and mentorship have gotten me through this challenging journey and I cannot thank you enough for that.

I would also like to thank the rest of the Tupling laboratory for their support. This thesis would not have been completed without the guidance of Dr. Dan Gamu. Dan, your encouragement and "tough love" helped me get my project off the ground and your work ethic and determination in the two years we were working together provided me with a role model to hold myself to. Thank you for friendship and support and making things interesting and fun at the lab. To Cat, Emma, Paige, Reilly, Brad, Gabbi, Val, and Khan, you made me feel less like a cog in the laboratory machine but more as a member of an extended family. Your friendship is greatly appreciated, and I wish you all the best in your future endeavours.

Finally, I would like to thank my family for their support and love. This has been a difficult but rewarding journey and you have stood by me with words of encouragement as I pursued this Master's degree. I am truly lucky to have such a large and supportive family.

Dedication

This thesis is dedicated to my father Jerry, mother Young Ju, uncle Joon, aunt Akane, and my dog Dol Dol. This experience has been at times stressful and difficult at times, but your love and support have helped get through this journey. This work is as much yours as it is mine.

Table of Contents

AUTHOR'S DECLARATION……ii

ABSTRACT……..iii

ACKNOWLEDGEMENTS……..v

DEDICATION……..vi

List of Tables…….....ix

List of Figures…….....x

Introduction……....1

Calcium Regulation and Thermogenesis …….....……..1

Adaptive Thermogenesis and Sarcolipin……..3

Duchene Muscular Dystrophy and Sarcolipin……..7

High Fat Feeding and mdx mice…….....10

Statement of the Problem……...11

Research Objectives……...11

Hypotheses……11

Methods……12

Experimental Animals……13

Experimental Design……..14

Whole Body Metabolic Rate Measures……..14

Whole body glucose tolerance tests……15

Tissue Collection……....15

Western Blot Analyses……...16

Statistical Analyses……....…16

Results……...17

Body Weight……..17

Adiposity and Anthropometric Measures……19

CLAMS Measurements…….....22

Metabolic Efficiency……...…....31

Glucose Tolerance Tests…….….27

Western Blotting Analysis……....…...……..29

Discussion…….31

Study Limitations……..42

Future Directions……..43

References……...45

Appendix A…….……59

Appendix B……..62

Appendix C……...…63

List of Tables

Table 1. CLAMS Measurements of Wild type (WT), *mdx* mice (*mdx*), and *mdx/Sln*-null mice (*mdx* SLNKO) Pre and Post Chow/HFD……..23

List of Figures

Figure 1. Experimental Diet Design; HFD: High Fat Diet; WT: wild type; mdx: murinic model of Duchenne muscular dystropohy……..14

Figure 2. Greater change in mass in WT with no differences in final bodyweight at sacrifice……..18

Figure 3. Total Food Consumption across an 8 week high fat diet (HFD) for wild-type (WT), *mdx*, and *mdx/Sln*-null mice……18

Figure 4. Fat pad mass, brown adipose tissue (BAT) weight, and adiposity index for chow fed control and HFD, wild type (WT), DMD mice (*mdx*), DMD Sln-null (*mdx* SLNKO) mice….20

Figure 5. Soleus and liver weights for chow fed control and HFD, wild type (WT), *mdx*, and *mdx/Sln*-null (mdx SLNKO) mice……..21

Figure 6. Metabolic efficiency (M.E) pre and post HFD ……26

Figure 7. Glucose tolerance curves and area under the curve (AUC) pre and post 8-week HFD ……...28

Figure 8. SLN expression in diaphragm (DIA)……30

Figure 9. UCP-1 expression in brown adipose tissue (BAT)……30

Introduction

Calcium Regulation and Thermogenesis

Calcium ions play a vital role in the physiology of living organisms. With respect to skeletal muscle, calcium regulates excitation-contraction coupling (ECC) (Stammers et al., 2015), apoptosis (Berchtold et al., 2000), secondary messenger signaling (Gailly, 2002), and energy expenditure (Bombardier et al., 2013a; Bombardier et al., 2013b). The precise regulation of intracellular free calcium ($[Ca^{2+}]_f$) is essential for proper skeletal muscle function and health. The sarcoplasmic reticulum (SR) is the primary organelle responsible for the dynamic control of both cytoplasmic and SR calcium levels in striated muscle (Martonosi and Pikula, 2003). The SR maintains a resting $[Ca^{2+}]_f$ within a concentration of 20-60 nM while maintaining a relatively greater luminal concentration creating a large Ca^{2+} gradient (1:10, 000) across the SR membrane (Schiaffino & Reggiani, 2011).

One of the integral SR membrane proteins that contributes to SR $[Ca^{2+}]_f$ regulation is the sarco(endo)plasmic reticulum Ca^{2+}-ATPase (SERCA) pump. SERCAs are a 110kDa membrane proteins responsible for the transport of calcium and the maintenance of $[Ca^{2+}]_f$ (MacLennan, Asahi, and Tupling, 2003). SERCA is a member of the protein family known as P-type ATPases, which utilize the energy from ATP to act as cation transporters (Toyoshima et al., 2000). The structural organization of SERCA is divided into three domains, a cytoplasmic head region, a transmembrane region containing the calcium binding sites, and luminal loops (Toyoshima et al., 2000; Toyoshima & Inesi, 2004; Stammers et al., 2015). The transmembrane region is comprised of 10 transmembrane domains (M1-M10) and the cytoplasmic head region is characterized by three cytoplasmic domains: the actuator domain, nucleotide binding domain, and the phosphorylation domain (Toyoshima et al., 2000). Although Ca^{2+}: ATP stoichiometry can be variable, the two calcium binding sites and one ATP binding site on SERCA corresponds to an

optimal coupling ratio of 2 Ca^{2+} for 1ATP hydrolyzed (Toyoshima, 2007). The two major conformational states of SERCA are the E1 and E2 states. Assuming an optimal ratio of 2 Ca^{2+} for 1 ATP hydrolyzed, the reaction cycle for SERCA mediated Ca^{2+} transport would proceed with 2 Ca^{2+} binding to the two Ca^{2+} binding sites on SERCA (Toyoshima & Inesi, 2004). The two major conformational states of SERCA are the E1 and E2 states. During the E1 state, the Ca^{2+} binding sites (M4, M5, M6, and M8 transmembrane proteins) have a high affinity for cytoplasmic calcium (Toyoshima, 2007). Once calcium ions are bound to SERCA in its E1 conformation, SERCA undergoes autophosphorylation by ATP at Asp351 at its phosphorylation domain forming a high energy phosphoprotein intermediate (E1P) (Toyoshima, 2007). SERCA transitions from E1P to a low energy phosphoprotein intermediate known as E2P (Toyoshima, 2007). The low energy state, E2P, is characterized by low SERCA calcium affinity, resulting in the release of calcium into the SR lumen (Toyoshima, 2007). Although Ca^{2+}: ATP stoichiometry can be variable, the two calcium binding sites and one ATP binding site on SERCA corresponds to an optimal coupling ratio of 2 Ca^{2+} for 1 ATP hydrolyzed (Toyoshima, 2007). This optimal ratio can be influenced by changes in physiological conditions, whereby the coupling ratio can be altered. A reduction in SERCA coupling ratio can occur as result of alterations in ADP/ATP ratios, $[Ca^{2+}]_f$, and sarcolipin (SLN) (Smith et al., 2002; Mall et al., 2006; Reis, Farage, & de Meis, 2002). There are three sources of reduced SERCA coupling ratio. First is a process known as a passive leak or uncoupled Ca^{2+} efflux whereby high concentrations of luminal SR Ca^{2+} results in the passive efflux of Ca^{2+} from the lumen of the SR back into the muscle cytoplasm, this occurs due to the binding of Ca^{2+} to SERCA in its E2 state before it can revert to its E1 state (Berman, 2001; de Meis, 2001b). The second is known as uncoupled ATPase activity, where the forward conformational transition from E1-Ca_2-P to E1-Ca_2-P is slowed down due to the high

luminal concentrations of Ca^{2+}, this increases the number of SERCA pumps in the E1-Ca_2-P state resulting in the cleavage of Pi before Ca^{2+} is translocated to the SR lumen (Berman, 2001; de Meis, 2001b). Finally, in a process known as slippage where the Ca^{2+} ion is prematurely released back into the muscle cytoplasm instead of the SR lumen during the conformational transition from E1-Ca^{2+}-P to E2-Ca^{2+}-P. A decrease in SERCA Ca^{2+} affinity when it is in the E1-Ca^{2+}-P is believed to be the cause of slippage (Smith et al., 2002; Berman, 2001). This reduction in affinity can be the result of high luminal Ca^{2+} concentrations or an interaction with SERCA regulatory proteins such as SLN and phospholamban (PLN). Although the three modalities of reducing Ca^{2+}: ATP stoichiometry are different, all three have the same result that most of the energy released from the hydrolysis of ATP is released as heat rather than the successful translocation of Ca^{2+} into the SR (Mall et al., 2006; Reis, Farage, and de Meis, 2002). This reduction in SERCA efficiency as a means to increase energy expenditure has been postulated as novel mechanism of skeletal muscle based adaptive thermogenesis.

Adaptive Thermogenesis and Sarcolipin

Adaptive thermogenesis refers to an increase in energy expenditure due to perturbations in either temperature or diet. It is important for a living organism to possess the ability to regulate energy expenditure during times of either food shortage or excess since it helps preserve energy stores and maintain body temperature. An inability to regulate either energy stores or body temperature can result in metabolic disorders such as obesity or even death. There are two mechanisms of adaptive thermogenesis: shivering thermogenesis and non-shivering thermogenesis.

Shivering thermogenesis involves the contraction of skeletal muscles, which generate metabolic heat (Cannon & Nedergaard, 2004). Skeletal muscle contraction/relaxation is a

process that is energy dependent requiring ATP at the level of the myosin ATPase and SERCA, two of the major energy consuming complexes during contraction. A complex series of both electrical and mechanical steps are involved in a process known as excitation-contraction (EC) coupling, a term linking the depolarization of the sarcolemma to the release of intracellular calcium from the SR, resulting in the formation of actin-myosin cross-bridges, and force production (Dulhunty, 2006). The formation of cross-bridges between actin and myosin by myosin ATPase, and the eventual re-uptake of calcium by SERCA, consume ATP and generate heat. Skeletal muscle represents the most direct avenue in which to increase energy expenditure either to help maintain body temperature or through exercise activity, prevent obesity. However, the elevated metabolic rate persists despite cessation of shivering during prolonged cold exposure, which underlies the importance of other mechanisms of thermogenesis, specifically non-shivering thermogenesis.

Non-shivering thermogenesis is the heat generated as result of mitochondrial proton leak seen in brown adipose tissue (BAT) (Cannon & Nedergaard, 2004). Mitochondrial proton leak occurs due to the presence of uncoupling protein 1 (UCP-1) which disrupts the proton (H^+) gradient by allowing protons to leak back into the mitochondrial matrix from the intermembrane space (Cannon & Nedergaard, 2004). The disruption of the proton motive force results in the uncoupling of ATP production from the movement of H^+ into the intermembrane space, as a result there is an increase in the break down and oxidation of carbon energy substrates (sugar, starch, protein, fat) in order to synthesize more reducing agents (NADH and $FADH_2$) in an effort to restore the disrupted mitochondrial H^+ gradient (Cannon & Nedergaard, 2004). Other isoforms of uncoupling proteins exist, UCP-2 is another uncoupling protein seen in BAT (Vidal-Puig et al., 1997), and UCP-3 a skeletal muscle-based isoform (Vidal-Puig et al., 2000) where all three

proteins share very similar sequence homologies (Feldmann, 2009). A study examining the effects of the ablation of UCP-1 in mice have found that at thermoneutrality (~30°C; a temperature at which no further compensatory thermogenesis mechanisms are needed to regulate body temperature), mice fed either a chow or a caloric dense high fat diet (HFD) are obese (Feldmann, 2009). The ability of UCP-1 to uncouple ATP production underlies an increase in energy expenditure which helps mitigate obesity pathogenesis. In a subsequent study, mice with overexpression of UCP-3 in their skeletal muscles were found to be protected from an obesity phenotype despite being fed a HFD (Son et al., 2004). These studies suggest that mice can be protected from obesity due to the existence of non-productive energy expending mechanisms. It has been suggested that other mechanisms may exist which help "waste energy" in an effort to attenuate excess caloric consumption and subsequent weight gain. One such mechanism may be SLN mediated slippage of Ca^{2+}.

SERCA function is regulated by several integral membrane proteins, including SLN (Asahi et al., 2003; Bal et al., 2012). SLN is a 31-amino acid protein, organized into three distinct domains, a cytoplasmic domain comprised of 7 hydrophilic amino acids, a hydrophobic 19 amino acid transmembrane domain, and a 6 amino acid luminal domain (MacLennan, Asahi, & Tupling, 2003). The expression of SLN protein in rodent tissue has been found to be abundant in the atria, the soleus (SOL), and the diaphragm (Vangheluwe et al., 2005a). SLN physically interacts with SERCA at its transmembrane domains (M4, M5, M6, and M8) (Toyoshima et al., 2000; Toyoshima & Inesi, 2004). The M4 and M6 transmembrane domains make up the calcium binding sites, whereby the physical presence of SLN can reduce SERCA calcium affinity and result in the premature release of calcium into the muscle cytoplasm instead of being translocated into the SR lumen during its catalytic cycle. Thus, SLN reduces the apparent affinity for Ca^{2+} in

both cardiac and skeletal muscle, as well as reducing maximal Ca^{2+} uptake activity (Toyoshima et al., 2000; Toyoshima & Inesi, 2004; Stammers et al., 2015). The uncoupling of ATP hydrolysis from SERCA Ca^{2+} uptake is another physiological role that SLN is responsible for. The amount of heat generated per molecule of ATP was increased as a result of SLN reconstitution in artificial membrane experiments (Smith et al., 2002). A greater rate of slippage may be the potential explanation for SLN ability to uncouple ATP hydrolysis from Ca^{2+} uptake. As mentioned in the first section, slippage occurs when Ca^{2+} ions are released prematurely while SERCA undergoes a conformational change between the E1 and E2 states. The unsuccessful translocation of Ca^{2+} from the muscle cytoplasm to the SR and the fact that ATP hydrolysis still occurs, results in reduced fraction of energy used to transport Ca^{2+} into the SR thereby reducing the coupling ratio (Ca^{2+} transported: ATP hydrolyzed) (Smith et al., 2002; Mall et al., 2006; de Meis, 2001a).

The interaction between SLN and SERCA has been postulated as a novel mechanism of diet induced thermogenesis (DIT), a form of non-shivering thermogenesis in response to excessive calorie consumption. In the soleus (SOL) of SLN ablated (*Sln*-null) mice, the apparent coupling ratios are higher than in WT counterparts (Bombardier et al., 2003b). A higher coupling ratio signifies a more energetically efficient transport of Ca^{2+} into the SR lumen, since Sln-null mice are able to transport a given amount of Ca^{2+} into the SR lumen at a lower energy cost. However, greater efficiency of Ca^{2+} transport can predispose *Sln*-null mice to obesity when fed an 8 week HFD (Bombardier et al., 2003b). This has been attributed to the absence of SLN mediated skeletal muscle adaptive thermogenesis and is characterized by greater weight gain, greater adiposity, and poorer glucose tolerance (Bal et al., 2012). In WT mice, a 3-5 fold increase in SLN is also observed in response to high fat feeding, further suggesting that SLN upregulation

is a mechanism of preventing excessive weight gain by promoting a decrease in SERCA energy efficiency (Bal et al., 2012; Bombardier et al., 2003a). The upregulation of SLN can also be observed in skeletal muscle disease states, such as Duchenne muscular dystrophy (Schneider et al., 2013).

Duchene Muscular Dystrophy and Sarcolipin

Duchenne muscular dystrophy (DMD) is an X-linked disease caused by a frame shift mutation in the dystrophin gene, abolishing the production of functional dystrophin protein (Blake et al., 2002; Bulfield et al., 1984; Dupont-Versteegden et al., 1994; Schneider et al, 2013; Sicinski et al., 1989). Dystrophin is a 427 kDa cytoplasmic protein that plays a key role in assembling several cytosolic and transmembrane proteins into the dystrophin associated glycoprotein complex (Blake et al., 2002; Bonilla et al., 1988; Garcia-Pelagio et al., 2011). Although the precise function of dystrophin remains unknown, its role in muscle function has been explored by its absence in animal models.

mdx mice (C57/BL10 background), the murine model of DMD, are genetically similar to DMD, with a nonsense point mutation centered on exon 23 of the dystrophin gene leading to an absence of dystrophin protein (Bonilla et al., 1988; Bulfield et al., 1984; Turner et al., 1988), and is a common model used to understand the DMD pathology (Bulfield et al., 1984; Turner et al., 1988). *mdx* mice display progressive diaphragm degeneration and cycles of skeletal muscle degeneration and regeneration analogous to DMD (Bonilla et al., 1988, Schneider et al., 2013; Turner et al., 1998; Willmann et al., 2009). The lack of dystrophin has been associated with membrane fragility as indicated by the high concentration of endogenous extracellular proteins albumin, IgG, and IgM, in the muscle cells (McGreevy et al., 2015; Mokhtarian et al., 1996). This has been attributed to the inability of cytoskeletal γ-actin to bind to the sarcolemma, leaving

the muscle vulnerable to mechanical stress and muscle damage (Dupont-Versteegden et al., 1994; Garcia-Pelagio et al., 2011; McGreevy et al., 2015). An absence of dystrophin has also been linked to membrane fragility which is associated with aberrant calcium handling and persistent increases in $[Ca^{2+}]_f$ (Culligan et al., 2002; McGreevy et al., 2015; Turner et al., 1988; Woods et al., 2004).

The increased influx of Ca^{2+} is initially started by mechanosensitive cation channels or stretch activated channels, preceding any signs of muscle damage and degeneration in young *mdx* mice, and is believed to be the primary source of Ca^{2+} entry into dystrophic muscle (Franco-Obregon Jr & Lansman, 1994). During subsequent contractile activity, transient membrane tears can occur which allow for localized influxes of calcium, a subsequent exocytotic transport of Ca^{2+} leak channels to the sarcolemma occurs which exacerbates the increased $[Ca^{2+}]_f$ (Turner et al., 1991). High $[Ca^{2+}]_f$ in skeletal muscle have been associated with degeneration and necrosis in *mdx* mice muscle (Gailly, 2002; Whitehead et al., 2006). Ca^{2+}-activated proteases, most notably calpains are responsible for promoting the degradation of numerous proteins which include membrane and cytoskeletal proteins. Calpain activity is higher in *mdx* mice than in WT mice, and remains elevated during periods of regeneration and degeneration (Spencer et al., 1995). The high $[Ca^{2+}]_f$ is also responsible for increased reactive oxygen species (ROS) production due to mitochondrial Ca^{2+} overload which impairs oxidative phosphorylation and normal mitochondrial Ca^{2+} handling (Kuznetsov, et al., 1998).

With respect to treatment, DMD at present has no known cure, however several treatment options have been explored. Genetic treatments include gene therapy aimed at either expressing a truncated, yet still in frame, dystrophin gene or restoring the dystrophin in its entirety (McGreevy et al., 2015). The goal of such therapy is to restore a functional gene or repair the gene through

targeted correction to restore dystrophin in DMD subjects (McGreevy et al., 2015). Pharmaceutical treatments have primarily focussed on glucocorticoids which help mitigate DMD pathology by reducing the breakdown of protein and increasing muscle mass (McGreevy et al., 2015). Another potential target of treatment has been the aforementioned calcium dysregulation observed in *mdx* mice. A recent study examining the downregulation of SLN in mdx utrophin knockout (utr -/-) mice, a more severe form of muscular dystrophy that mimics human DMD, saw reduced pathophysiology and improved muscle function (Voit, 2017). One of the major characteristics of mdx mice is their high energy expenditure and inability to meet that energy demand, possibly due to cycles of skeletal muscle degeneration and regeneration (Radley et al., 2014). As a result, dietary interventions have been explored in addition to pharmaceutical and genetic treatment options. Potential dietary interventions aimed specifically at protein/amino acid supplementation have been examined extensively (Radley et al., 2007). However, their benefits remain mixed as some studies have shown potential benefits while others have shown no improvement (for review see Radley et al., 2007). Due to the high energy demand of mdx mice, interventions using a caloric dense HFD have been explored as a therapeutic option (Radley-Crabb et al., 2011).

High fat feeding and mdx mice

Previous work has shown that mdx mice are in a constant state of caloric deficit, where their energy intake is unable to meet their energy demands (Radley-Crabb et al., 2011; Radley-Crabb et al., 2014). This calorie deficit has been postulated as an exacerbating complication of the mdx disease, as muscles and protein must be broken down and used as energy substrates to meet mdx energy demands. As a result, Radley-Crabb (2011) fed mdx mice a calorie rich HFD (32% kcal from fat) in an effort to compensate for high energy expenditure to mitigate the

severity of mdx mice dystropathology (Radley-Crabb et al., 2011). After 24 weeks, the bodyweights of the mdx mice did not significantly change after consuming a HFD, whereas WT mice had significantly higher body weights (Radley-Crabb et al., 2011). The differences in bodyweight between mdx and WT mice could not be accounted for by differences in food consumption or by differences in the amount of activity (Radley-Crabb et al., 2011). The body composition comparisons between the two strains revealed that the mdx mice also had significantly smaller fat pad masses in contrast to WT. High fat feeding also had a profound impact on the dystropathology of mdx mice improving muscle fibre integrity (Radley-Crabb et al., 2011). It should be noted that the diet used in the study was not using a Westernized high fat diet. Although, the diet (32% kcal from fat) is relatively higher in fat in comparison to the chow diet given (5% from fat; 22/5 Rodent Diet (w) 8640; Harlan Teklad, Madison WI), it is considerably lower than the Westernized high fat diet (42% kcal from fat; product TD 88137; Harlan Teklad, Madison, WI) used in previous studies (Bombardier, 2010; Gamu, 2012). Pilot work has shown that *mdx* mice fed a Westernized HFD are still protected from obesity. Even with the higher percentage HFD, mdx mice had lower weight gain in comparison to WT mice, had lower adiposity, and displayed lower metabolic efficiency. Potential mechanisms of higher energy expenditure in mdx mice have often focussed on the cycles of degeneration and regeneration and protein synthesis (Dupont-Versteegden et al., 1994; Mokhatrian et al., 1996; Radley et al., 2007; Radley-Crabb et al., 2014). However, protection against obesity as a possible consequence of SLN upregulation in mdx mice has not been explored, despite SLN's established role in adaptive thermogenesis.

Statement of the Problem

The increase in SLN and protection from diet-induced obesity in mice has lead us to believe that SLN may be a major protective mechanism against diet-induced obesity in mdx mice. To investigate the potential protective role of SLN against obesity in *mdx* mice, a transgenic line of *mdx/Sln*-null mice were examined and compared with *mdx* and WT mice.

Research Objectives:

General Objective:

- Determine if SLN mediated diet induced thermogenesis is a major mechanism of obesity protection in mdx mice.

Specific Objectives:

i) To compare relative sarcolipin levels in *mdx* and WT mice after HFD.
ii) To determine if *mdx/Sln*-null mice are protected against obesity.
iii) To determine if differences in VO_2, activity Levels, and food Consumption have any effect on obesity protection in *mdx* mice.

Hypotheses:

i) SLN levels in *mdx* mice will be higher in comparison to WT mice. Since HFD increases the expression of SLN, SLN will increase in both strains, but the SLN levels will be higher in mdx mice due to its already high expression in skeletal muscle.
ii) In comparison to WT mice, *mdx* mice will be protected from obesity after consuming a Western high fat diet, which will be denoted by lower body weight, lower adiposity, and lower blood glucose measures.

iii) *mdx*/*Sln*-null mice will not be as obese as WT, but will not be protected from obesity after consuming a Western high fat diet with a higher body weight, higher adiposity, and higher blood glucose measures in comparison to *mdx* mice.

iv) Energy expenditure in *mdx* mice will be higher in response to the elevated levels of sarcolipin and thermogenesis as a result of high fat feeding, with no significant differences in activity levels.

Methods

Experimental Animals

mdx mice were purchased from Jackson Laboratories with intention of breeding an *mdx* SLN and *mdx/Sln*-null colony. The *mdx* mice were crossed with a *Sln*-null colony maintained at the University of Waterloo in order to create a line of *mdx/Sln*-null mice. Animals for the proposed project were hemizygous mdx males and WT littermates. A wild type comparison was considered a necessary group in order to observe the degree of protection from obesity in *mdx* mice and *mdx/Sln*-null mice. For the duration of the study, animals were individually housed in an environmentally controlled room on a regular 12:12 light dark cycle and allowed access to food and water *ad libitum*. Analyses were conducted on soleus and diaphragm, since SLN are normally observed in these tissues. All experiments were reviewed and approved by the University of Waterloo Animal Care Committee in accordance with the Canadian Council on Animal Care.

Experimental Design

WT, *mdx*, and *mdx/Sln*-null were randomly assigned to dietary treatments as outlined below (Figure 1). The experimental diets were administered for a period of 8 weeks and comprised of ad libitum access to water and HFD (42% of kcal from fat, product TD 88137; Harlan Teklad, Madison, WI). Body mass was measured on a weekly basis during the administration of the experimental diets. The experimental design included 8-week chow fed control animals, whose data is included in Appendix A.

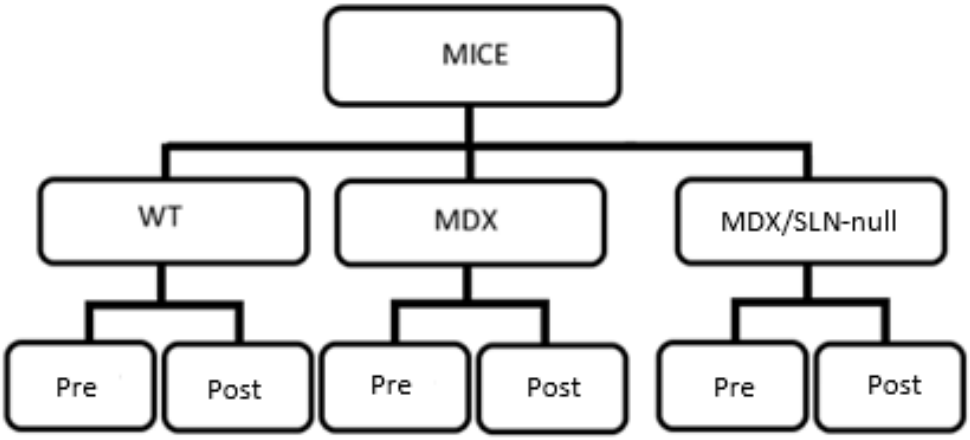

Figure 1. Experimental Diet Design; Pre: pre-HFD; Post: post-HFD; WT: wild type; mdx: murinic model of Duchenne muscular dystrophy.

Whole-Body Metabolic Rate Measures

WT, *mdx*, and *mdx/Sln*-null littermates were acclimated in clear plastic cages for one week and given ad libitum access to water and rodent chow (22/5 Rodent Diet (w) 8640; Harlan Teklad, Madison WI), prior to commencing whole-body metabolic measurements. Whole-body metabolic measurements were made using a Comprehensive Laboratory Animal Monitoring System (CLAMS; Oxymax Series; Columbus Instruments, Columbus OH). Animals were housed individually in clear plexiglass cages (20 cm x 10 xm x 12.5 cm) in a room that was temperature controlled to (~22° Celsius), on a reverse light dark cycle and allowed access to water and powdered food (as above) *ad libitum*. Twenty-four hours were allocated to acclimate the mice to the CLAMS before commencing measurements and data collection for a period of 24 hours thereafter. CLAMS measurements were completed two times during the same week, these measurements will be taken both before and after the experimental diets. Those mice who were allocated to the HFD will be given powdered high-fat food while in the CLAMS instead of the standard chow diet. The percent O_2 and CO_2 gas levels of the cages (20 cm x 10 cm x 12.5 cm) were measured periodically between reference readings of room air and were used to compute

the O2 consumption (VO2) of the animal and used to calculate the daily metabolic rate. Relative VO_2 measurements will be recorded in ml O_2/kg/hr, whereas absolute VO_2 will factor in the body weights of the animals and be recorded as ml O_2/hr. In addition to metabolic rate, the CLAMs are equipped with a scale for monitoring mass of food consumed over time. There were also X and Z activity sensors for monitoring ambulatory activity (dual beam) counts (when 2 adjacent X axis beams are broken in succession) in addition to both total activity and rearing activity.

Whole-Body Glucose Tolerance Tests

Pre- and post-diet Whole body glucose tolerance tests (GTT) were conducted on all mice as outlined in Gamu (2012). Mice were fasted overnight (16 hrs); following the fast, each mice was administered an intraperitoneal injection of 20% D-Glucose (1g/1kg body mass), a 5-10ul sample of venous blood was drawn from the tail vein and blood glucose measured using a glucometer (Contour Next; Bayer Diabetes Canada). Timepoints of blood glucose measure occurred immediately before intraperitoneal injection, after 30, 60, and 120 minutes post-injection.

Tissue Collection

Prior to commencing tissue collection, mice were placed on a four hour fast. Experimental animals were euthanized by cervical dislocation, the soleus and diaphragm were collected. All tissue samples were frozen in liquid N_2 and stored at -80°C for future analyses. The retroperitoneal and epididymal fat pads were excised, cleaned of extraneous tissue and weighed. The weights of the epididymal, and retroperitoneal fat pads were used to calculate the adiposity index as:

(Sum of epididymal and retroperitoneal pad masses/body mass) X 100

Western Blotting Analysis

Soleus and diaphragm muscles from WT, mdx, and *mdx/Sln*-null mice were collected and homogenized 10:1 (volume/weight). Brown adipose tissue (BAT) was also collected and later homogenized 4:1 (volume/weight). Proteins will be separated in glycine based SDS-PAGE (13% Total AB6/AB3) for SLN. Separated proteins will be transferred onto a nitrocellulose membrane for SLN and a PVDF membrane for UCP-1 and immunoprobed with their corresponding primary antibodies and subsequently immunoprobed with the appropriate horseradish peroxidase-conjugated secondary antibodies. Luminata Forte™ was used to detect SLN and UCP-1 antigen-antibody complexes. Quantification of optical densities was determined using GeneTools (Syngene, MD, USA) and all values were normalized to whole protein content.

Statistical Analyses

One-way ANOVAs were used to test for differences between WT, *mdx*, and *mdx/Sln*-null groups with respect to changes in body weight post-HFD. A two-way ANOVA, examining the factors of genotype and diet (pre/post-HFD), was used to detect differences in body weight, food consumption, all CLAMS measures, anthropometric measures such as fat pad masses, muscles and liver weights, as well as protein expression and glucose area under the curve (AUC) across all three genotypes, pre- and post-HFD. Analyses were performed using Statistica 12 (Statsoft. Inc., Tulsa, OK, USA). Data are presented as means ± SE. The significance level was set at 0.05, and when appropriate, a Newman-Keuls post hoc test was used to compare specific means.

RESULTS

Body Weight and Food Consumption

Pre-diet body weight was higher ($P < 0.0001$) in *mdx* and *mdx/Sln*-null mice in comparison to WT mice with no differences observed between *mdx* groups (Fig.2b). In response to the HFD, body weight of all three genotypes increased significantly ($P < 0.0001$), with WT gaining more mass versus both *mdx* and *mdx/Sln*-null at week 5 ($P < 0.03$), week 6 ($P < 0.02$), week 7 ($P < 0.02$), and week 8 ($P < 0.01$) of the HFD (Fig. 2a). However, at the time of sacrifice (8 weeks Post-HFD), there were no differences in body weight between genotypes post-HFD (Fig.2b). Weight gain was also not different at any time point between high fat fed *mdx* and *mdx/Sln*-null mice (Fig. 2a).

Total food consumption was measured across all 8 weeks of the HFD, and across all three genotypes. The total food consumption was significantly higher ($P < 0.05$) in *mdx* mice in comparison to WT and *mdx/Sln*-null mice (Figure 3). There was no difference ($P = 0.99$) in food consumption between WT and *mdx/Sln*-null mice.

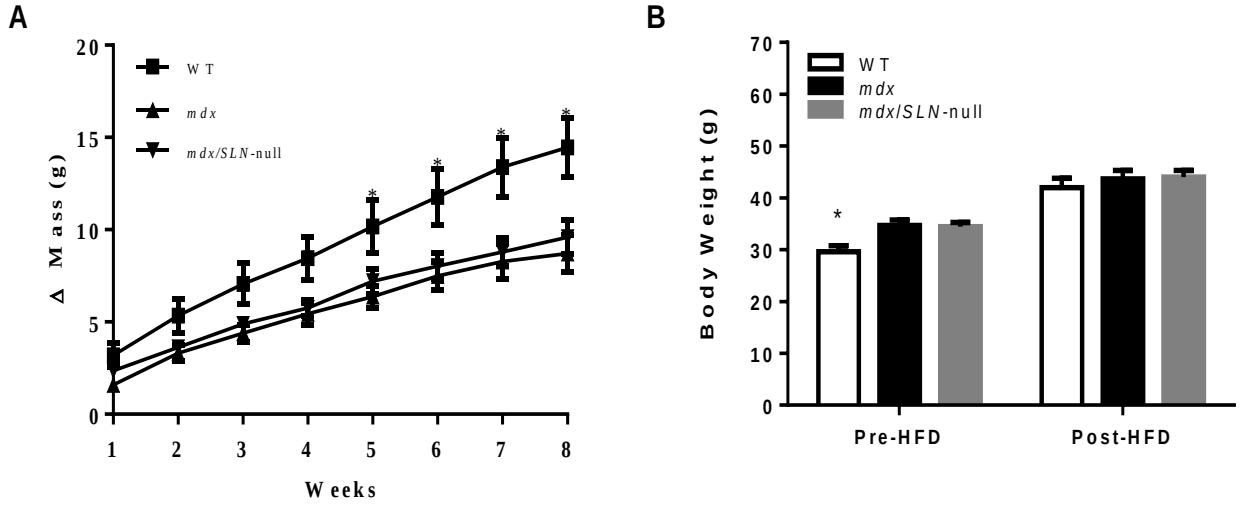

Figure 2. Greater change in mass in WT with no differences in final bodyweight at sacrifice. A) Change in body mass of wild-type (WT), *mdx*, and *mdx/Sln*-null mice during 8 weeks of a high-fat diet (HFD). B) Pre- and Post-HFD bodyweights of WT, *mdx*, and *mdx/Sln*-null mice. Values are mean ± S.E. * Significantly different than corresponding *mdx* and *mdx*/*Sln*-null ($P < 0.05$). (WT: n = 9, *m*dx: n = 12, *mdx*/*Sln*-null; n = 8)

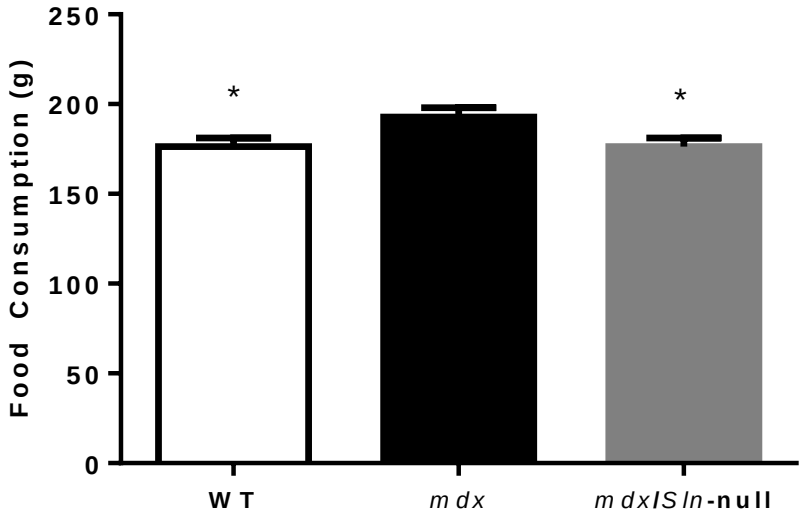

Figure 3. Total Food Consumption across an 8 week high fat diet (HFD) for wild-type (WT), *mdx*, and *mdx/Sln*-null mice. *Significantly different from *mdx* mice. Values are mean ± S.E. * Significantly different than *mdx* ($P < 0.05$). (WT: n = 9, *m*dx: n = 12, *mdx*/*Sln*-null; n = 8)

Adiposity and Anthropometric Measures

After consuming an 8-week high fat diet, an interaction ($P < 0.02$) was observed with *mdx/Sln*-null mice having higher epididymal fat pad masses, higher BAT fat pad masses, and a higher adiposity index compared to *mdx* mice post-HFD (Figure 4). An interaction close to statistical significance ($P = 0.07$) was observed with *mdx/Sln*-null mice having greater retroperitoneal fat pad masses in comparison to *mdx* mice post-HFD. Planned comparisons (Newman-Keuls) revealed that WT mice had greater epididymal fat pad masses ($P < 0.001$; Figure 4a), greater retroperitoneal fat masses ($P < 0.001$; Figure 4b), and higher adiposity index ($P < 0.01$; Figure 4d) than *mdx/Sln*-null and *mdx* mice regardless of diet. Post-HFD WT mice had greater ($P < 0.001$) BAT masses than post-HFD *mdx/Sln*-null and *mdx* mice, there were no differences between chow fed WT and *mdx* ($P = 0.45$) and *mdx/Sln*-null mice ($P = 0.24$). A main effect of diet ($P < 0.0001$) was observed with fat pad masses and adiposity indexes being higher post-HFD compared to chow.

When comparing soleus weights between groups, there were significant main effects of diet and genotype with soleus mass being heavier post-HFD compared with pre-HFD ($P < 0.02$) and in both *mdx* and *mdx/Sln*-null mice compared with WT ($P< 0.0001$; Figure 5a). The same main effects were observed when soleus weights were expressed as a percentage of bodyweight (Figure 5c). With respect to liver weights, an interaction ($P < 0.05$) was observed with WT mice having greater post-HFD liver weights than *mdx* and *mdx/Sln*-null mice, despite having the lowest liver mass pre-diet (Figure 5b). When liver weights were normalized to body weight, an interaction ($P < 0.05$) was observed with greater liver % BW post-HFD in WT mice and *mdx/Sln*-null mice in comparison to *mdx* mice, despite WT mice starting out with a low liver % BW and mdx/*Sln*-null mice having similar liver % BW pre-diet to mdx (Figure 5d). Planned

comparisons (Newman-Keuls) revealed that post-HFD *mdx/Sln*-null mice had significantly ($P < 0.05$) higher liver % BW in comparison to post-HFD *mdx* mice, with no differences ($P = 0.79$) observed when compared to WT mice. Planned comparisons further revealed a significant increase in liver % BW post-HFD in WT mice in comparison to pre-HFD ($P < 0.02$). An interaction that was close to statistical significance ($P = 0.08$) was observed with greater liver % BW in HFD fed *mdx/Sln*-null mice in comparison to chow controls. No differences were observed between HFD and chow fed *mdx* mice ($P = 0.93$).

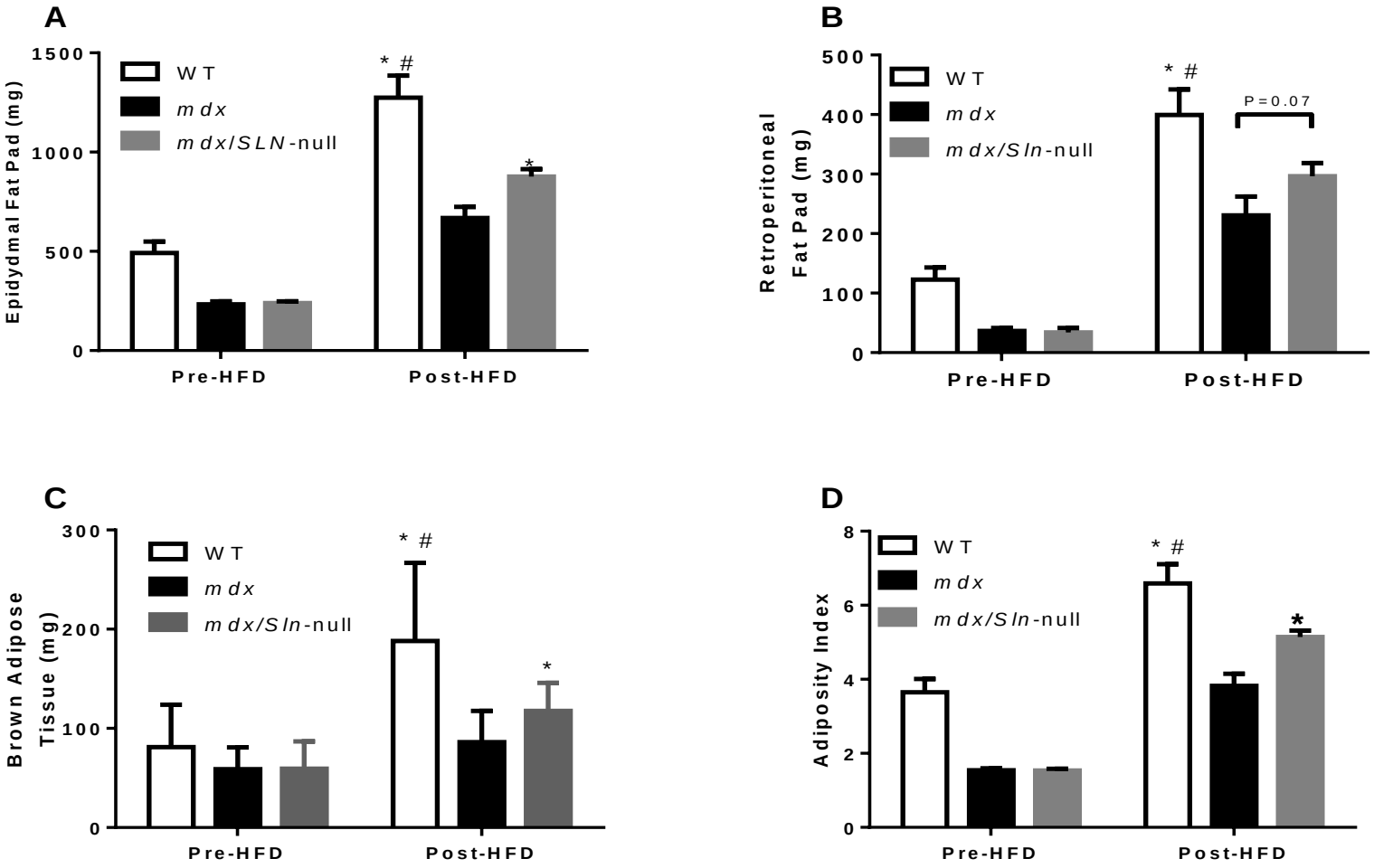

Figure 4. Fat pad mass, brown adipose tissue (BAT) weight, and adiposity index for chow fed control and HFD, wild type (WT), *mdx* mice, *mdx/Sln*-null mice. (A) epididymal fat pad mass; (B) retroperitoneal fat pad mass; (C) BAT mass; (D) adiposity index. All showed a main effect ($P < 0.0001$) of diet with HFD > Chow and main effect ($P < 0.0001$) of genotype with WT > *mdx* SLNKO > *mdx*. *Significantly different ($P < 0.05$) than *mdx*. #Significantly different from *mdx/Sln*-null. Values are means±SE (N=11 for WT Pre-HFD, N=9 for WT Post-HFD, N=13 for *mdx* Pre-Chow, N=12 for *mdx* Post-HFD, N=8 for *mdx* mdx/*Sln*-null Pre-HFD, N=8 for *mdx*/*Sln*-null Post-HFD).

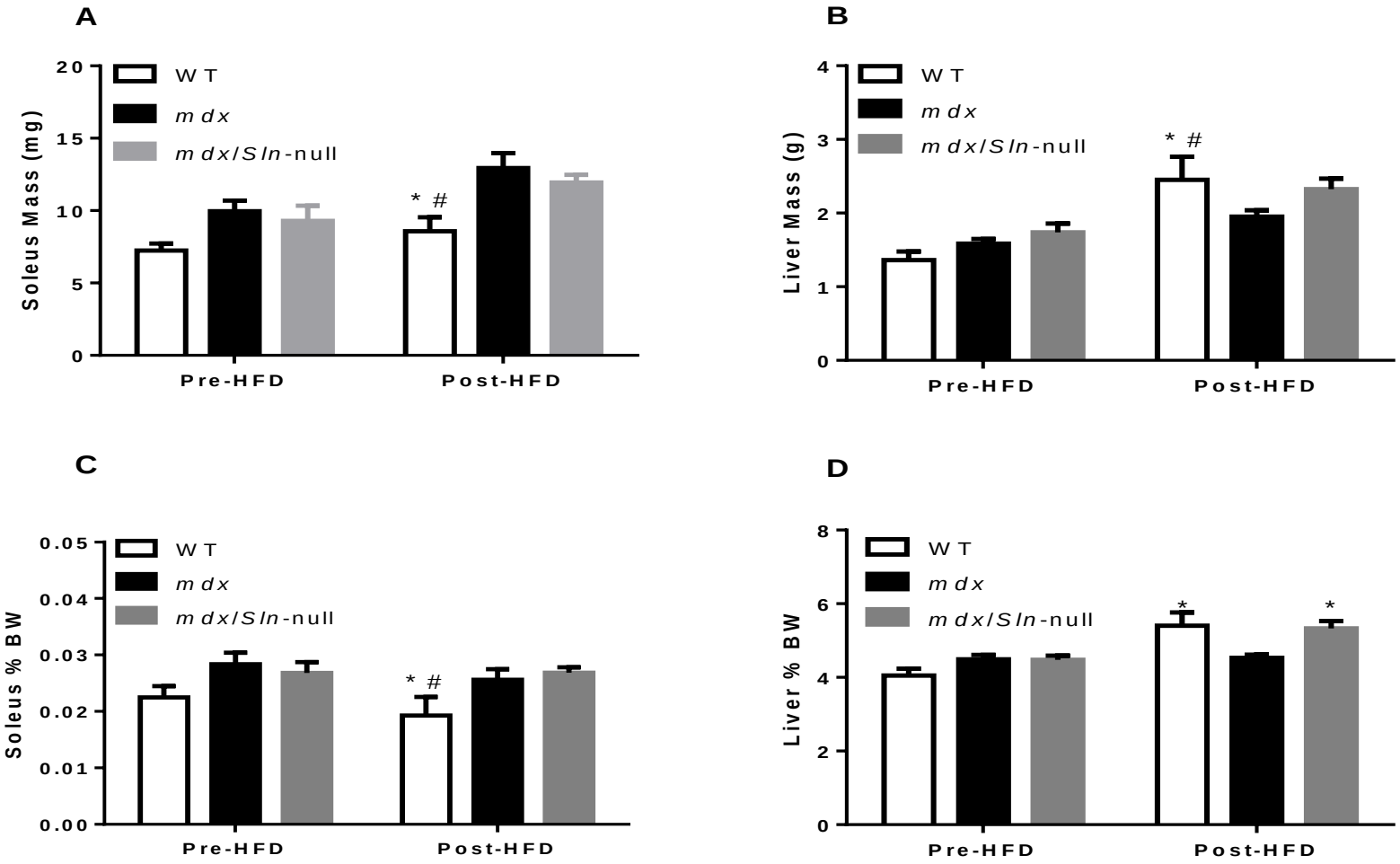

Figure 5. Soleus and liver weights for chow fed control and HFD, wild type (WT), *mdx*, and *mdx/Sln*-null mice. (A) Soleus mass (main effect of genotype: $P < 0.0001$ *mdx*/ *mdx/Sln*-null > WT; main effect of diet: $P < 0.02$, HFD > Chow); (B) liver weight (main effect of diet: $P < 0.0001$, HFD > Chow); (C) soleus % BW (main effect of genotype: $P < 0.004$, *mdx*/ *mdx/Sln*-null > WT; main effect of diet: $P < 0.05$); (D) liver % BW (main effect of diet: $P<0.01$, HFD > Chow). * Significantly different from mdx ($P < 0.05$). #Significantly different ($P < 0.05$) than *mdx/Sln*-null mice. Values are means±SE (N=11 for WT Pre-HFD, N=9 for WT Post-HFD, N=13 for *mdx* Pre-Chow, N=12 for *mdx* Post-HFD, N=8 for *mdx* mdx/*Sln*-null Pre-HFD, N=8 for *mdx*/*Sln*-null Post-HFD).

CLAMS Measurements

CLAMS data are presented in Table 1. Pre-HFD relative total daily VO_2, relative waking VO_2 and relative sleeping VO_2, were significantly lower in *mdx/Sln*-null mice compared to both WT ($P < 0.01$) and *mdx* ($P < 0.02$) mice. No differences ($P > 0.5$) in these pre-HFD relative VO_2 measures were observed between *mdx* and WT mice. However, for all pre-HFD absolute (ml O_2/hr) VO_2 measures (i.e. total, waking and sleeping), values were lower in WT mice compared with both *mdx* ($P < 0.0001$) and *mdx/Sln*-null ($P < 0.01$) mice. No differences ($P > 0.1$) in these pre-HFD absolute VO_2 measures were observed between *mdx* and *mdx/Sln*-null mice. Planned comparisons revealed that *mdx* mice had 4% greater pre-HFD absolute daily VO_2 compared to *mdx/Sln*-null mice, but the difference was not significant ($P = 0.26$). Pre-HFD total and dual cage activity were higher ($P < 0.001$) in WT mice in comparison to *mdx* and *mdx/Sln*-null mice. Both pre-diet total and dual beam activity were not different ($P > 0.05$) in *mdx* versus *mdx/Sln*-null mice.

Following the 8-week HFD, relative total daily, waking and sleeping VO_2 were higher ($P < 0.05$) in *mdx* mice in comparison to both WT and *mdx/Sln*-null mice. Furthermore, post-HFD relative total daily, waking and sleeping VO_2 were higher in WT compared to *mdx/Sln*-null mice. A main effect of diet ($P < 0.0001$) was also observed with all three animal groups having lower relative total daily, waking and sleeping VO_2 post-HFD compared with pre-HFD. In contrast to relative VO_2, all absolute VO_2 values were higher ($P < 0.05$) post-HFD in comparison to pre-HFD. Similar to relative VO_2, all absolute VO_2 values were higher ($P < 0.0001$) in *mdx* mice in comparison to WT and *mdx/Sln*-null mice, with the exception of absolute sleeping VO_2, which was not different ($P = 0.24$) between *mdx* and *mdx/Sln*-null mice. Food intake (g) also demonstrated a main effect ($P < 0.0001$) of diet with post-HFD intake being lower than pre-

HFD. No significant differences were found in food consumption between the three groups either pre- or post-HFD. The smaller quantity (g) of high fat food eaten by all three groups of mice was calculated to have the same amount of metabolizable energy as the standard rodent chow eaten during pre-HFD CLAMS measurements (3.0 kcal/g for standard chow versus 4.5 kcal/g for the HFD; Table 1). For activity levels there was a main effect ($P < 0.01$) of genotype, whereby WT mice had greater total activity and dual beam activity than both *mdx* and *mdx/Sln*-null mice both pre- and post-HFD. There was no main effect of diet for either total activity ($P = 0.67$) or dual beam activity ($P = 0.79$). Finally, a main effect of diet ($P < 0.0001$) was found for all three-respiratory exchange ratio (RER) values with pre-HFD values being higher than post-HFD values. There was also a main effect of genotype ($P < 0.05$) for sleeping RER, with WT mice having higher values than both *mdx* and *mdx/Sln*-null mice.

Table 1. CLAMS Measurements of Wild type (WT), *mdx*, and *mdx/Sln*-null mice Pre and Post-HFD

	Pre			Post		
	WT	*mdx*	*mdx/Sln*-null	WT	*mdx*	*mdx/Sln*-null
Body Weight (g)	30.6 ± 1.3	34.5 ± 1.1#	34.8 ± 0.77#	44.6 ± 2.4*	44.3 ± 1.7*	45.3 ± 1.1*
Waking VO_2 (ml O_2/kg/hr)	3457± 55	3461 ± 55	3250 ± 59#$	2909 ± 52*	3349 ± 113*#	2805 ± 42*#$
Sleeping VO_2 (ml O_2/kg/hr)	2668 ± 80	2781 ± 68	2630 ± 26#$	2587± 62*	2733 ± 59*#	2456 ± 46#$
Total Daily VO_2 (ml O_2/kg/hr)	3203 ± 51	3240 ± 55	3038 ± 70#$	2838 ± 52*	3135 ± 76*#	2689 ± 37*#$
Food Intake (g)	3.83 ± 0.31	3.97 ± 0.22	4.20 ± 0.25	2.47 ± 0.19*	2.57 ± 0.24*	2.57 ± 0.31*
Metabolizable Energy (kcal)	11.49 ± 0.93	11.9 ± 0.66	12.61 ± 0.76	11.13 ± 0.19*	11.55 ± 0.52*	11.56 ± 0.49*
Total Activity	10776 ± 718	7624 ± 215#	7072 ± 174#	9852 ± 450	8257 ± 209#	7750 ± 132#
Dual Beam Activity	3632 ± 349	2601 ± 238#	2515 ± 198#	3358 ± 198	2728 ± 134#	2471 ± 128#

Waking VO_2 (ml O_2/hr)	103 ± 4.7	119 ± 2.8#	113 ± 1.2#	116 ± 6.3*	140 ± 5.1*#	126 ± 2.7*#$
Sleeping VO_2 (ml O_2/hr)	79 ± 3.8	95 ± 2.0#	91 ± 1.2#	104 ± 6.4*	119 ± 5.1*#	111 ± 3.5*
Daily VO_2 (ml O_2/hr)	95 ± 4.1	111 ± 2.3#	105 ± 1.4#	116 ± 5.8*	137 ± 4.7*#	118 ± 5.4*$
Awake RER	0.921 ± 0.007	0.920 ± 0.009	0.916 ± 0.014	0.815 ± 0.007*	0.806 ± 0.007*	0.794 ± 0.011*
Sleep RER	0.908 ± 0.009	0.891 ± 0.007	0.8907 ± 0.005	0.798 ± 0.009*	0.774 ± 0.009*	0.768 ± 0.013*
Total RER	0.912 ± 0.010	0.906 ± 0.009	0.906 ± 0.01	0.807 ± 0.008*	0.794 ± 0.009*	0.784 ± 0.01*

Main effect of diet (Pre < Post) for Body Weight (P<.0001). Main effect of diet (Pre > Post) Waking, Sleeping, and Daily VO_2 (P<0.0001), Food Intake (P<0.0001), Total Activity (P<0.05), Dual Beam Activity (P<0.05), and Waking, Sleeping, Total RER (P<0.0001). Main effect of genotype (WT>*mdx* and *mdx/Sln*-null) for sleeping RER (P<0.05).*Significantly different from Pre (P<0.05). #Significantly different from WT. $ Significantly different than mdx. VO_2, oxygen consumption, RER, respiratory exchange ratio. Values are Mean ± SEM (N=9 for WT, N=12 for mdx, N=8 for mdx SLNKO)

Metabolic Efficiency

Metabolic efficiency (M.E) was calculated by dividing the change in body weight by the amount of energy derived from either chow or high fat diet converted to kJ. An interaction ($P < 0.0001$) was found, with WT mice having significantly greater metabolic efficiency post-HFD than *mdx* and *mdx/Sln*-null mice (Figure 6). Planned comparisons revealed a trend ($P = 0.07$) towards higher metabolic efficiency in *mdx/Sln*-null mice in comparison to mdx mice post-HFD (Figure 8). There were no differences in metabolic efficiency pre-HFD.

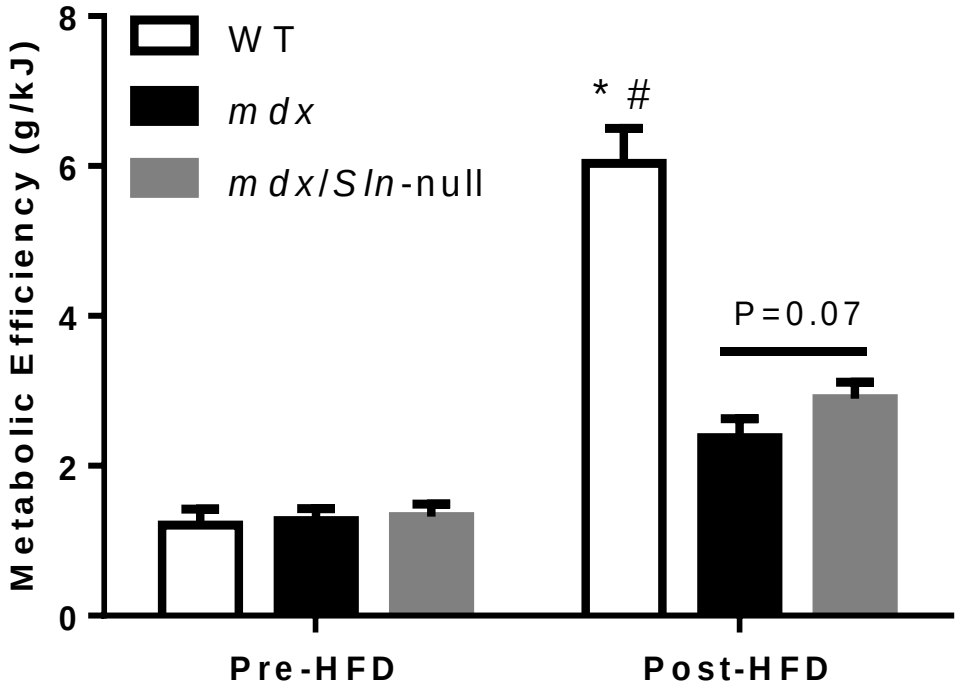

Figure 6. Metabolic efficiency (M.E) pre- and post- HFD. M.E. increases in response to high fat diet (main effect of diet: $P < 0.0001$). Trend towards higher metabolic efficiency in *mdx/Sln*-null vs *mdx* mice (P=0.07). *Significantly greater than mdx mice ($P < 0.0001$). # Significantly greater than *mdx/Sln*-null mice ($P < 0.0001$). Values are mean ± S.E. (N=8 for WT, N=12 for mdx, N=8 for mdx SLNKO)

Glucose tolerance tests

GTT were performed on WT, *mdx*, and *mdx/Sln*-null mice pre- and post-HFD (Figure 5a). There were large differences between pre- and post-HFD responses with the glucose values being lower ($P < 0.001$) at all time points during pre-diet tests compared with post-diet tests in WT (Fig. 7a) and at two time points in *mdx/Sln*-null mice (Fig. 7b). There were no differences observed between pre- and post-diet responses with *mdx* mice (Fig. 7a). A trend towards an interaction ($P = 0.06$) was observed showing greater glucose intolerance (higher blood glucose levels) post-HFD in *mdx/Sln*-null mice compared with WT (Fig. 7b) and *mdx* mice (Fig. 7c). Planned comparisons (Neuman-Keuls) between *mdx* and *mdx/Sln*-null at the 60 and 120 min time points showed that *mdx/Sln*-null were more ($P < 0.05$) glucose intolerant post-HFD in comparison to *mdx* mice. A comparison of pre-diet values revealed no significant differences between *mdx* and *mdx/Sln*-null mice.

Whole glucose excursions after an intraperitoneal injection of glucose are a good representation of glucose tolerance. Another index of glucose tolerance is the glucose area under the curve (AUC), which represents the total amount of blood glucose throughout the two-hour glucose tolerance test, where greater values will represent poorer glucose tolerance. When expressed as an AUC, an interaction was observed ($P< 0.02$) with *mdx/Sln*-null mice showing greater blood glucose post-HFD in comparison to mdx and WT mice (Fig. 7d). Planned comparisons (Neuman-Keuls) showed that post-HFD blood glucose levels were greater ($P < 0.05$) in *mdx/Sln*-null mice in comparison to *mdx mice*; WT mice tended ($P = 0.08$) to have lower AUC values post-HFD in comparison to *mdx/Sln*-null mice.

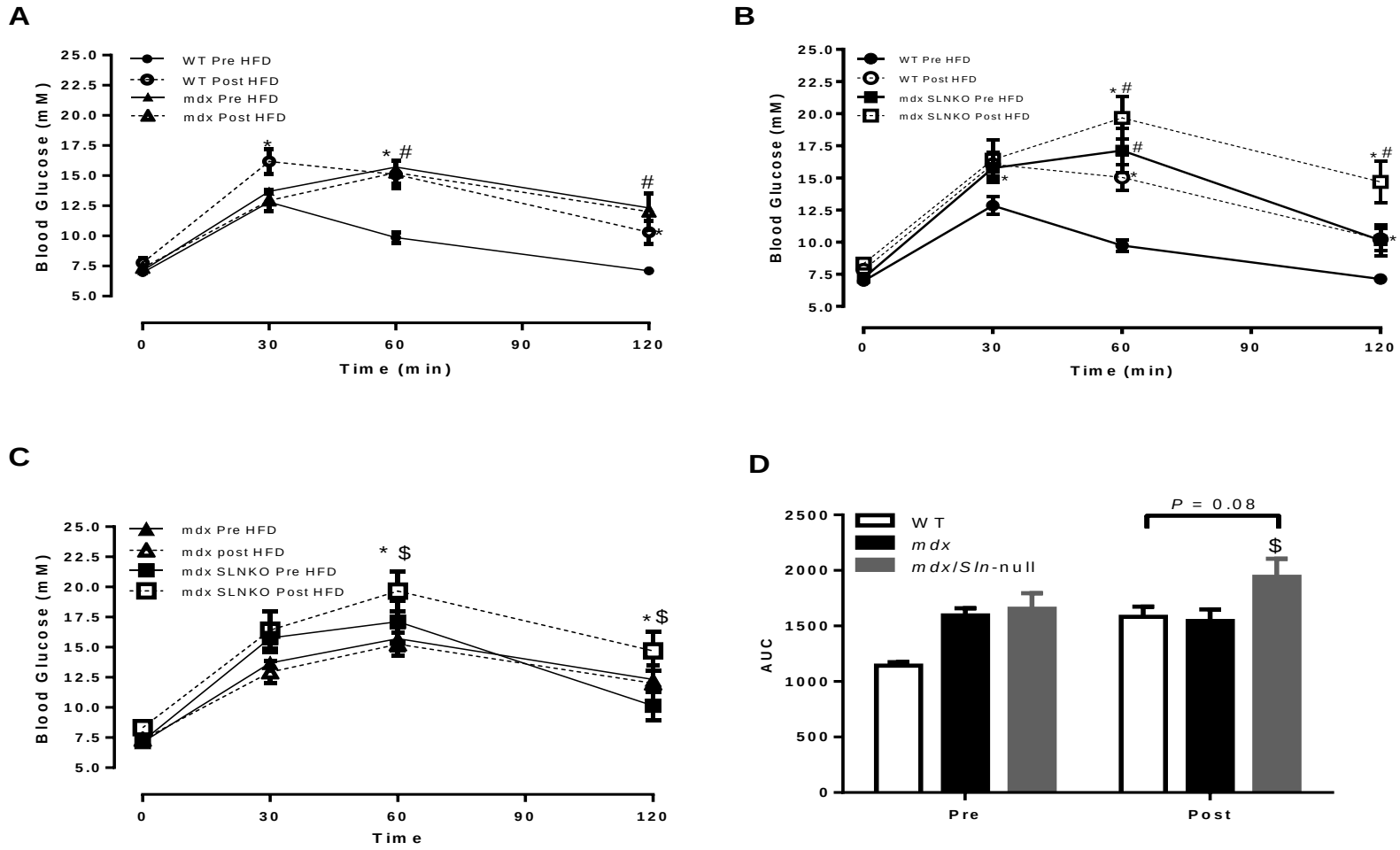

Figure 7. Glucose tolerance curves and area under the curve (AUC) pre and post 8-week HFD. (A) Wild type (WT) vs. *mdx*, (B) WT vs. *mdx/Sln*-null, (C) *mdx* vs *mdx/Sln*-null, (D) Glucose AUC. Main effect of genotype ($P < 0.0001$), WT < *mdx*/ *mdx*/Sln-null. Main effect of time ($P < 0.0001$), 0 < 120 < 30 < 60. *Significantly different from Pre ($P < 0.05$). # Significantly different from WT ($P < 0.05$). $ Significantly different from *mdx* ($P < 0.05$). Values are Mean ± SEM (N=11 for WT, N=12 for *mdx*, N=8 for *mdx*/*Sln*-null)

Western Blotting Analysis

Comparisons between chow fed WT, *mdx* mice, and *mdx/Sln*-null revealed that SLN is elevated in the *mdx* diaphragm ($P < 0.0001$) by a factor of 2, SLN was not detected in the *mdx/Sln*-null samples (Figure 8). Due to "technical issues", SLN expression could not be accurately detected in the soleus. Comparisons between HFD fed WT and *mdx* mice shows that SLN remains elevated in the *mdx* diaphragm ($P < 0.02$) by a factor of 1.5. Interestingly, SLN levels decreased ($P < 0.05$) in the diaphragms of mdx mice post-HFD. UCP-1 was elevated ($P < 0.02$; Figure 9) post-HFD across all three genotypes, WT (30%), *mdx* (29%), and *mdx/Sln*-null (25%). However, UCP-1 content was not different ($P > 0.05$; Figure 9) between WT, *mdx*, and *mdx/Sln*-null post-HFD.

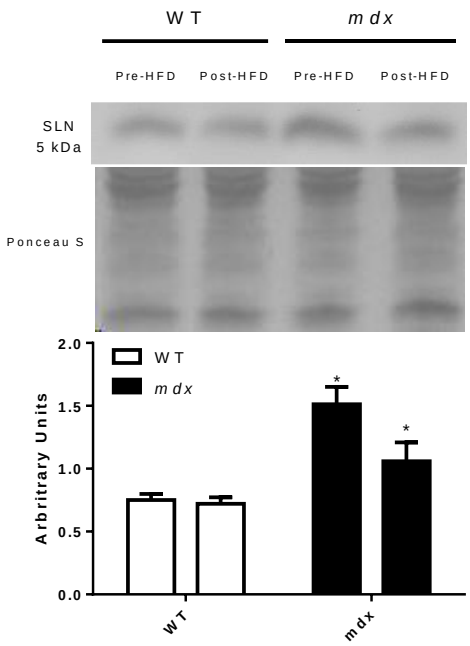

Figure 8. SLN expression in diaphragm (DIA). SLN is higher in mdx diaphragm by a factor of 2. Post-HFD the SLN expression remained higher in mdx diaphragm in comparison to WT mice by factor of 1.75. *Significantly different than WT ($P < 0.05$). Values are mean ± S.E (N=9 for WT Pre-HFD, N=8 for WT Post-HFD, N=9 for *mdx* Pre-HFD, N=9 for *mdx* Post-HFD).

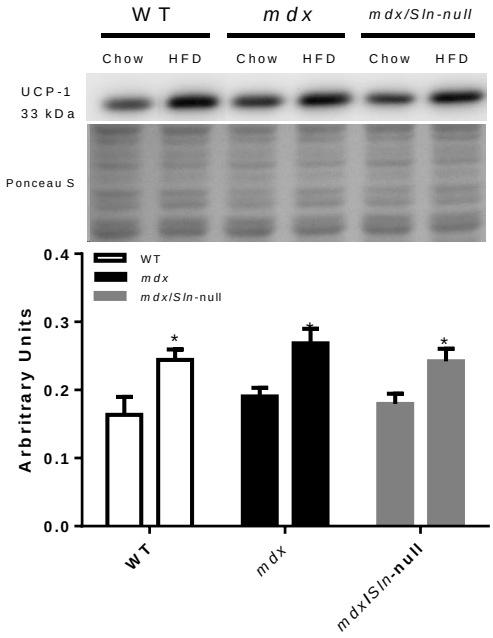

Figure 9. UCP-1 expression in brown adipose tissue (BAT). Post-HFD, UCP-1 expression increased in WT (30%), *mdx* (29%), and *mdx/Sln*-null (25%). No significant differences between all three genotypes. *Significantly different from Chow ($P < 0.05$). Values are mean ± S.E (N=8 for WT Pre-HFD, N =8 for WT Post-HFD, N=8 for *mdx* Pre-HFD, N=8 for *mdx* Post-HFD, N=8 for *mdx/Sln*-null Pre-HFD, N=8 for *mdx/Sln*-null Post-HFD).

Discussion

This study set out to assess the role of SLN in providing protection against high fat diet induced obesity in *mdx* mice. The main findings of this study were: 1) SLN content in the diaphragm was higher in *mdx* mice compared to WT mice; 2) *mdx/Sln*-null mice had statistically significantly greater adiposity post-HFD, despite a non-statistical significant increase in body weight in comparison to mdx mice; 3) in accordance with the ablation of SLN, *mdx/Sln*-null mice demonstrated a lower whole body metabolic rate in comparison to *mdx* mice. Altogether these results further support SLN's thermogenic role, wherein the absence of SLN is a major mechanism of diet induced obesity in *mdx/Sln*-null mice.

A previous study saw an upregulation of SLN in the diaphragm and soleus of *mdx* mice (Schneider et al., 2013). As hypothesized, there was a significant difference in the expression of SLN between WT and *mdx* mice, with a 2-fold higher expression in the diaphragm of *mdx* mice vs WT mice (Fig. 8). In relation to the Schneider study, a similar difference was observed with mdx diaphragm expressing a 3-fold increase in comparison to WT mice (Schneider et al., 2013). Schneider et al. (2013) also observed a 10-fold difference in the expression of SLN in the soleus muscle of *mdx* mice in comparison to WT mice. This finding could not be corroborated during this study due to the lack of viable results that could be systematically discerned due to technical issues. However, the finding of higher expressions of SLN in the diaphragm of *mdx* mice helps corroborate the finding that SLN is upregulated in mdx mice.

A novel finding was that after consuming a high fat diet, SLN in the diaphragm declined in mdx mice by 30% (Fig. 8). This decrease in SLN expression may seem paradoxical as SLN has been found to increase in soleus muscles of high fat fed animals (Bombardier, 2010). However, the thermogenic contribution of diaphragm to skeletal muscle non-shivering

thermogenesis is at this time unknown and the expression of SLN in diaphragm post-HFD has not been shown to change (Bal et al., 2012). This was corroborated in this study as SLN expression in the diaphragm of WT mice did not change after an 8-week HFD (Fig. 8). The upregulation in SLN seen in the muscles of *mdx* has been proposed as a contributing factor to it's pathology (Schneider et al., 2013). However, SLN upregulation has also been proposed as a compensatory mechanism to combat *mdx* pathology by upregulating utrophin, a dystrophin homologue, through increased NFAT translocation to the muscle nucleus via calcineurin activation (Fajardo, 2015). A previous study examining the quadriceps of *mdx* mice post-HFD have found that those muscles have significantly reduced myofibre necrosis when measured as a % of cross sectional area (% CSA), almost half the amount observed in chow fed *mdx* mice (Radley-Crabb et al., 2011). Furthermore, voluntarily exercised mdx mice on a high fat diet were able to run 50% further than their chow counterparts (Radley-Crabb et al., 2014).

CLAMs data from this study revealed total and dual beam activity was always lower in *mdx* mice and *mdx/Sln*-null mice in comparison to WT mice with mdx mice having greater movement than *mdx/Sln*-null mice (Table 1). Despite no statistical significance, post-HFD mdx mice saw an 8.3% increase in cage activity; there was also an 9.5% increase in cage activity observed in *mdx/Sln*-null mice. Two possible explanations may account for the increase in activity in both mdx strains, (1) the high fat diet may be better suited to meeting the energy demands of the *mdx* and *mdx/Sln*-null mice and/or (2) the high fat diet may have altered the phospholipid membrane composition and reduced calcium leak from the SR/ER. Diets that are high in saturated fat and cholesterol can change the composition of the phospholipid membrane of skeletal muscles, particularly the incorporation of a higher percentage of saturated fatty acids in the muscle phospholipid membrane (Janovska et al., 2010). Alterations in the form of

increased saturated fatty acids and cholesterol in the phospholipid membrane of the SR have been found to reduce membrane fluidity thus reduce the rate of Ca^{2+} leak from the SR/ER (Vangheluwe et al., 2005). This reduction in Ca^{2+} could help reduce the dystropathology of *mdx* mice and improve muscle function. This could also help explain the decline of SLN in the diaphragm of HFD fed *mdx* mice. Calcium dysregulation in the muscle is one of the chief symptoms of Duchenne muscular dystrophy which contributes to its pathology (Franco-Obregon & Lansman, 1994; Turner, et al., 1991; Whitehead et al., 2006). The findings of the present study would suggest that the high fat diet may cause a compensatory decrease of SLN in mdx mice that could alleviate muscle necrosis and improve function. Furthermore, SLN expression remained upregulated despite a 30% decrease in comparison to pre-diet mdx mice. This suggests that despite the decline in SLN expression in response to high fat feeding, the already upregulated expression of SLN in mdx mice is large enough to maintain a significant difference in comparison to WT mice thereby maintaining SLN mediated thermogenesis in *mdx* mice. A future study may be needed to examine if the same decrease in expression occurs in mdx soleus due to it's role in adaptive thermogenesis. These findings pose interesting future questions for high fat diet's therapeutic role in DMD treatment.

The ablation of sarcolipin results in a more efficient pumping of calcium into the SR (Bal et al., 2012), thus it was hypothesized that an overexpression of SLN would result in higher levels of SERCA uncoupling, increased energy expenditure, and protection against obesity (Maurya et al., 2015). After consuming an 8-week high fat diet, mice overexpressing SLN (SLN^{OE}) were found to have lost weight and maintain a normal metabolic profile in comparison to WT mice and KO mice despite consuming significantly more calories than WT mice (Maurya et al., 2015). For this study, it was hypothesized that the upregulated expression of SLN in *mdx*

mice would enhance adaptive thermogenesis and increase protection against diet-induced obesity and glucose intolerance. The body weights of WT and *mdx* mice were different pre-HFD with *mdx* mice (33.8 ± 0.58g) being heavier than WT mice (29.9 ± 0.73g). The significant differences in body weight pre-HFD can be attributed to pseudohypertrophy, a compensatory muscle hypertrophy due to muscle necrosis and replacement by connective tissue and fat in the muscles of *mdx* mice (Mokhatarian et al., 1996; Connolly et al., 2001; Coulton et al., 1988; Anderson et al, 1987). In contrast, post-HFD body weights of WT and *mdx* mice were not significantly different (43.1 ± 1.98g for WT vs 43.7 ± 1.98g for *mdx*) in accordance to previous findings which also observed no differences in final body weights (Radley-Crabb et al., 2011). The most likely explanation for a lack of a difference in bodyweight between WT and *mdx* mice after an 8-week high fat diet is the increase in body fat in the WT mice (Figure 4d).

Despite the lack of differences in final body weight post-HFD, as hypothesized WT mice experienced a 31% increase in body weight over the 8-week period. This demonstrates that the WT mice experienced greater weight gain (13.1 ± 1.15g) than *mdx* (9.0 ± 1.0g) or *mdx/Sln*-null (9.59 ± 0.92g) mice from week 2 of the high fat diet until its eventual completion (Fig. 2a). The weight gain observed in WT mice was in accordance with other studies examining weight gain over an 8-week high fat diet (Li et al., 2000; Collins et al., 2004; Bombardier, 2010). However, the weight gains observed in *mdx* mice were higher post HFD (171%) than the previously reported 137% increase (Radley-Crabb et al., 2014). One potential explanation could be a difference in the composition of the diets. The present study used a Western diet (TD 88137; Harlan Teklad, Madison, WI; 21.2% fat by weight; 42% of kcal from fat) whereas Radley-Crabb (2011) used a different high fat diet (SF06-040, Specialty Feeds, Glenn Forest, WA;16% fat by weight and 32% of kcal from fat) (Radley-Crabb, 2014). Furthermore, the diets varied in their

fatty acid profiles, with the Westernized high diet having 61.8% comprised of saturated fatty acids, whereas the high fat diet only had 3.26% composition of saturated fatty acids (Radley-Crabb et al., 2011). Higher fat composition may have exacerbated weight gain in the *mdx* mice, thereby resulting in greater weight gain. This has been demonstrated across a variety of species and with various diets, with specific diets causing some species to gain more weight in comparison to other diets (Buettner et al., 2007). These findings further support that the composition of diet plays an important role in the manifestation of obesity.

The ablation of sarcolipin has been shown to increase the efficiency of the SERCA pumps, predisposing SLN ablated mice to obesity after consuming a high fat diet (Bombardier, 2010). In this study, it was hypothesized that the ablation of SLN in *mdx* mice would have similar effects to *mdx/Sln*-null mice, namely that they would be more susceptible to diet induced obesity and glucose intolerance when compared to *mdx* mice. Despite no statistical difference in weight gain between *mdx* and *mdx/Sln*-null mice, food consumption was significantly lower in *mdx/Sln*-null mice in comparison to *mdx* mice (Fig. 3). Thus, the *mdx/Sln*-null mice gained the same amount of weight as *mdx* mice despite consuming less of the high fat diet. The ablation of SLN blunts adaptive thermogenesis, resulting in higher metabolic efficiency, wherein less of the energy derived from ATP is dissipated as heat but rather stored and used as meaningful work. Higher metabolic efficiency makes it less likely that excess energy consumed from diet will be expended through thermogenic means, but instead stored as adipose tissue. Previous studies have shown that mice with increased metabolic efficiency, either through weight loss or the ablation of thermogenic proteins such as UCP-1, are more likely to gain weight and exhibit greater obesity (Maclean et al., 2004; Feldmann et al., 2007). Furthermore, *Sln*-null mice have exhibited enhanced metabolic efficiency, which was reflected in greater weight gain and adiposity in

comparison to WT mice (Rowland et al., 2016). As hypothesized, *mdx/Sln*-null mice displayed higher metabolic efficiency post-HFD than *mdx* mice (Fig. 6). Thus, *mdx/Sln*-null mice were less able to expend the extra calories ingested from the HFD in comparison to *mdx* mice which predisposed them to high fat diet induced obesity. One possible explanation for the difference in food consumption between *mdx* and *mdx/Sln*-null mice may be related to inflammatory cytokines. Elevated levels of TNF-α, IL1β, and IL-6 are a hallmark of *mdx* skeletal muscle dystropathology (Tidball et al., 2005). TNF-α, IL1β, and IL-6 have been found to increase leptin, a hormone that suppresses hunger and reduces food consumption, in a dose dependent manner (Saraff et al., 1997). A previous study examining the pathological impact of SLN ablation in *mdx* skeletal muscles found reduced myofiber area and greater muscle fibre breakdown with elevated serum creatine kinase (Fajardo, 2015). Due to enhanced mdx pathology, it is probable that *mdx/Sln*-null mice would also experience elevated levels of TNF-α, IL1β, and IL-6, wherein the fat expression and serum levels of leptin would increase and thereby reduce food consumption.

The expansion of adipose tissue due to increased deposits of triacyglycerides (TAGs) into adipose depots is a common feature seen in rodent models of obesity (West and York, 1998). This study observed an approximately 2.8-9 fold higher fat pad weights in WT, *mdx*, and *mdx/Sln*-null mice post-HFD compared to chow fed counterparts (Fig. 3). Liver weights were significantly greater post-HFD across all three genotypes. When expressed as a percentage of body mass, the livers of high fat diet-fed animals comprised a larger percentage of body mass, particularly the WT and *mdx/Sln*-null mice (Fig. 5d). Interestingly, despite consuming a high fat diet, the liver % BW of *mdx* mice did not change. This may be an indication of *mdx* mice resistance to a high fat diet, since greater deposits of lipids in the liver is a common feature of obesity (Kontani et al., 2005; deLany and West, 2000).

As hypothesized, *mdx/Sln*-null mice had greater epididymal fat pad masses compared to mdx mice. The calculated adiposity index was highest in the WT mice displaying greater obesity than that of *mdx* and *mdx/Sln*-null mice. The adiposity index of *mdx/Sln*-null mice was significantly higher ($P < 0.01$) than mdx mice, thereby making *mdx/Sln*-null mice more obese. Despite differences in animal models, these results remain consistent with previous findings of increased high fat diet-induced obesity in SLN ablated mice (Bombardier, 2010). No differences in fat pad masses, BAT, or adiposity were observed between *mdx* and *mdx/Sln*-null pre-diet. These findings corroborated previous work (Bombardier, 2010; Gamu, 2012).

Although mdx mice moved considerably less than WT mice, their waking VO_2 was not significantly different prior to commencing their high fat diets. The higher waking, sleeping, and total daily VO_2 (mlO_2/kg/hr) observed in *mdx* mice post-HFD supports the hypothesis that *mdx* mice are better protected from obesity compared to WT mice due to increased SLN expression and increased energy expenditure. In contrast, pre-diet total daily VO_2 and waking VO_2 were significantly higher in *mdx* mice compared to *mdx/Sln*-null mice possibly due to the greater cage movement seen in *mdx* mice. There was a significant increase in absolute total daily VO_2 across all three genotypes post-HFD where mdx mice had greater absolute VO_2 values in comparison to WT mice. This is consistent with findings that mdx mice have greater energy expenditure than WT mice (Radley-Crabb et al., 2014). *Mdx* mice had greater waking and daily VO_2 with respect to *mdx/Sln*-null mice, again supporting the hypothesis that mdx mice are better protected from obesity due to increased energy expenditure. Interestingly, there was no difference in all three absolute VO_2 values between *mdx/Sln*-null and WT mice. This may seem paradoxical as weight gain and adiposity were significantly lower in *mdx/Sln*-null mice in comparison to WT mice. However, *mdx/Sln*-null mice moved considerably less than WT mice, thus *mdx/Sln*-null mice

have similar absolute VO_2 values as WT mice despite a lower cage activity which would denote greater energy expenditure.

Unexpectedly, the post-HFD sleeping VO_2 values of *mdx* did not decrease substantially in comparison to *mdx/Sln*-null or WT mice. When examining absolute sleeping VO_2 values, an 18% increase in basal metabolism in *mdx* ($P < 0.001$) and *mdx/Sln*-null ($P < 0.02$) mice was observed with no significant difference between the two strains suggesting there was no difference in basal metabolism. The lack of a difference in basal metabolism is consistent with previous findings examining WT and *Sln*-null mice, which saw no difference in basal metabolism post-HFD (Bombardier, 2010). The ablation of SLN reduced the SERCA contribution to ATP consumption in *Sln*-null mice (Bombardier, 2010). As such *mdx/Sln*-null mice would experience a similar effect. Thus, other adaptive thermogenic mechanisms must be involved in increasing the energy expenditure of both mdx and *mdx/Sln*-null mice, with these mechanisms playing a greater role in *mdx/Sln*-null mice due to a decrease in SERCA energy consumption. One such mechanism is UCP-1 in the brown adipose tissue, which has been identified as a powerful agent of adaptive thermogenesis (Lowell and Spiegelman, 2000). Post-HFD weights of BAT were significantly higher ($P < 0.05$) in *mdx/Sln*-null mice in comparison to *mdx* mice and significantly lower than WT mice. This would suggest that when compared to *mdx* mice, the increase in energy expenditure in *mdx/Sln*-null mice could be accounted for by increases in UCP-1 expression. However, despite significant increases in UCP-1 expression post-HFD, there was no significant difference in UCP-1 expression across all three genotypes (Figure 7). Thus, the increase in energy expenditure and the differences in adiposity could not be accounted for by the increased expression of UCP-1 nor could it explain the increased basal metabolism of both *mdx* and *mdx/Sln*-null mice. However, as the name implies, UCP-1 is not the

only uncoupling protein, UCP-3 is another mitochondrial uncoupling protein found in BAT and skeletal muscle. UCP-3 expression has been upregulated in response to high fat feeding and obesity (Schrauwen et al., 2001), although it's importance to thermogenesis is tentative at best as UCP-3 ablation studies have not shown a significant reduction in whole body energy expenditure (Vidal-Puig et al., 2000; Hoeks et al., 2006). Previous studies have shown that *mdx* mice do not have significant differences in the expression of UCP-3 in comparison to WT mice (Perceival et al., 2013). However, this was observed under chow fed conditions and there has yet to be a study examining the effect of HFD on the expression of UCP-3 of *mdx* mice. It can be speculated that HFD could potentially increase the expression of UCP-3 in mdx and/or *mdx/Sln*-null mice, thereby increasing their basal metabolic rate. Another consideration is the upregulation of phospholamban (PLN) in BAT tissue. PLN is an SLN homologue and possesses a similar capacity to uncouple Ca^{2+} transport from ATP hydrolysis (Frank et al., 2000). PLN has been found to be upregulated in the BAT tissue of both WT and *Sln*-null mice fed a HFD (Bombardier, 2010). Although not examined in this study, there is a possibility that the expression of PLN may have been upregulated in *mdx* and *mdx/Sln*-null causing an increase in basal metabolism which may account for the lack of a difference in UCP-1 expression and higher BAT mass in *mdx/Sln*-null mice. Another possible explanation for the similar basal metabolism of mdx and *mdx/Sln*-null mice is the upregulation of catecholamines. Norepinephrine (NE) and epinephrine (E) have been found to be elevated in the HFD fed Sln-null mice (Bombardier, 2010). It has been established that an increase in sympathetic nervous system (SNS) activity augments energy metabolism and thermogenesis (Maickel et al., 1967; Cannon and Nedergrad, 2003). *mdx* mice have been found to have heightened sympathetic nervous activity (Chu, 2002), however there is very little literature regarding the levels of catecholamines in *mdx* mice.

Although not examined in the present study, hindlimb perfusion experiments in rats have demonstrated the ability of NE to stimulate skeletal muscle VO_2 potentially through increased activity of the Na+-K+ ATPase (Clausen, 1986; Shiota and Masumi, 1988). Thus, it is possible that higher catecholamine levels in *mdx/Sln*-null mice post HFD could partly account for the higher absolute basal VO_2.

Despite not knowing the precise mechanisms underlying lower total whole metabolic rate in *mdx/Sln*-null mice, the fact remains that *mdx/Sln*-null mice were more obese and glucose intolerant than HFD fed *mdx* littermates. Glucose tolerance responses in WT and *mdx* mice pre-HFD were consistent with previous studies with *mdx* mice demonstrating greater glucose intolerance than WT mice (Stapleton, 2014). After high fat feeding, WT mice exhibited reduced glucose tolerance comparable to *mdx* mice; *mdx* mice exhibited no difference from pre-HFD glucose tolerance. In contrast, glucose tolerance responses between *mdx* and *mdx/Sln*-null mice were not different pre-HFD; however as hypothesized, *mdx/Sln*-null mice demonstrated a greater glucose intolerance than *mdx* and WT mice post-HFD (Figure 5). The greater glucose intolerance observed in WT mice is consistent with previous high fat feeding studies that saw a comparable increase in blood glucose following the consumption of a 42% Westernized diet (Li et al., 2000; Bombardier, 2010; Gamu, 2012). While not directly assessed here, the observed glucose intolerance in both WT and *mdx/Sln*-null mice may be reflective of reduced skeletal muscle insulin stimulated uptake of glucose. It has been demonstrated that elevated levels of plasma free fatty acids (FFA) play a major role in reduced skeletal muscle insulin sensitivity (Kashyap et al., 2003, Roden et al., 1996). However, if elevated FFAs played a role in glucose intolerance, *mdx* mice should have experienced a greater glucose intolerance after high fat diet which was not observed. Interestingly, *mdx/Sln*-null mice experienced a greater severity of glucose intolerance

in comparison to *mdx* mice. A possible explanation for this may be related to cytoarchitecture of mdx and *mdx/Sln*-null mice. Glucose metabolism involves the translocation of glucose transporter 4 (GLUT4) from the cytoplasm to the sarcolemma either due to insulin dependent or independent signaling pathways. An intact cell membrane and cortical actin system is needed to allow the fusion of GLUT4-loaded vesicles with the sarcolemma, in addition to a functioning microtubule (MT) network for long-distance vesicle transport. *Mdx* mice membranes are characterized by their fragility due to the lack of dystrophin, leaving their muscles vulnerable to mechanical stress and damage. The lack of dystrophin compromises the integrity of the cell membrane, thereby disrupting the proper translocation of GLUT4 to the sarcolemma. Utrophin, a dystrophin homologue, is highly upregulated in the membrane of mdx muscles as a compensatory protein to make up for the lack of dystrophin in the cytoarchitecture. *Mdx/Sln*-null mice have been found with lower expression of utrophin, which further compromises membrane integrity as evidenced by lower muscle CSA% and higher creatine kinase in comparison to mdx mice (Fajardo, 2015). Thus, the worsened membrane integrity of *mdx/Sln*-null mice may further inhibit the translocation of GLUT4 to the sarcolemma resulting in greater glucose intolerance. Other potential mechanisms may contribute to the greater glucose intolerance in *mdx/Sln*-null mice compared to *mdx* mice. Adiponectin, an insulin sensitizing agent, levels may have been reduced due to increased obesity (Arita et al., 2000). Also, there may have been a greater inflammation of adipose tissue related to the hypertrophy of adipocytes causing an elevation of inflammatory cytokines such as TNF-α (Guilherme et al., 2008). As evidence by the greater adiposity of *mdx/Sln*-null mice following high fat feeding, it would seem that both of these mechanisms may a play a role in a greater glucose intolerance, as both mechanisms have been shown to decrease glucose uptake (Dycke et al., 2006; Guilherme et al., 2008).

Summary and Conclusions

In summary, this study demonstrates that the ablation of SLN in *mdx* mice resulted in greater obesity and glucose intolerance potentially due to the lower daily energy expenditure seen in *mdx/Sln*-null mice compared to *mdx* mice following a HFD. Furthermore, *mdx* mice were found to be protected from obesity due to greater daily energy expenditure seen in mdx mice in comparison to WT mice. Western blotting revealed that SLN expression was 2-fold higher in the diaphragm of *mdx* mice compared to WT mice, the elevated levels of SLN was still observed in HFD fed *mdx* mice despite a 30% decline. Much like previous studies from our laboratory, the ablation of SLN *mdx* mice manifested in greater adiposity and poorer glucose tolerance after the consumption of an 8-week high fat diet. Glucose tolerance did not change after HFD in *mdx* mice, whereas *mdx/Sln*-null mice glucose tolerance was more severe than WT and *mdx* mice, possibly due to a decrease in membrane integrity brought upon by a possible decline in utrophin expression. Taken altogether, these data suggest that SLN plays an important role in adaptive thermogenesis in *mdx* mice.

Limitations

There were a variety of limitations for this study. First, this study was unable to provide a successful detection of SLN in soleus despite our best efforts. Previous studies performed in our laboratory have done so successfully and such information would have provided more meaningful insight into the role of SLN in adaptive thermogenesis in *mdx* mice. This may have been the result of technical issues and/or the quality of the soleus muscle prep which should be addressed in future projects. Secondly, the role of UCP-3 in thermogenesis was not assessed, thus their role with respect to enhanced basal metabolism in *mdx* and *mdx/Sln*-null mice is only speculative. Thirdly, efforts were made to maintain consistent environmental conditions,

however one cohort of mice were housed in a high humidity (80-85% relative humidity) environment due to a faulty environmental control system within that wing of the central animal facility. As the animals were already into their diets, dehumidifiers were used to try and mitigate the elevation in humidity. However, dehumidifiers were found to be noisy and had to be cleared of excess water every 12 hours. The added noise from the humidifiers and effort to empty them may have elicited a greater stress response in these animals affecting food consumption and VO_2 measurements.

Future Directions

With relevance to adaptive thermogenesis, it would be interesting to examine the relative contribution of UCP-1 to the increased basal metabolism seen in *mdx/Sln*-null mice. Although, the expression of UCP-1 was not different between *mdx* and *mdx/Sln*-null mice, BAT weights were significantly higher in *mdx/Sln*-null mice. The ablation of UCP-1 has been shown to cause diet-induced obesity (Feldmann et al., 2009), it would be of interest to observe if BAT played a larger role in elevating basal metabolism post-HFD in *mdx/Sln*-null mice versus mdx mice. A future study examining *mdx/Sln*-null mice with their BAT surgically removed could provide insight into this. Other potential thermogenic mechanisms, such as UCP-3, should be explored as they may explain the elevation in sleeping VO_2 observed in both *mdx* and *mdx/Sln*-null mice.

The role of catecholamines in enhancing basal metabolism of both *mdx* and *mdx/Sln*-null should be examined more thoroughly. NE and E levels should be measured in future high fat feeding studies to observe whether elevations may have caused subsequent increases in VO_2 Post-HFD. This interest is due to the potential role of catecholamines in augmenting fat lipolysis/de novo synthesis via AMPK activation in skeletal muscle (Dulloo et al., 2004). Furthermore, elevated catecholamines act on adipocytes resulting in the activation of G couple

protein receptors in adipocytes and the stimulation of adenylyl cyclase leading to the elevation of cyclic AMP, ultimately increasing the blood levels of NEFA, through the activation of hormone sensitive lipase, which is known to cause glucose intolerance and insulin resistance (Roden et al., 1996). A comparative chow group will need to be done as well, as information regarding catecholamine levels in mdx mice has yet to have been reported. Also, it would be beneficial to examine NEFA levels as well as mdx mice did not experience poorer glucose tolerance after a HFD.

The role of cytoarchitecture with respect to glucose tolerance should be examine more thoroughly. The loss of dystrophin has been associated with a subsequent worsening of glucose tolerance due to an inability to properly translocate GLUT4 to the sarcolemma of mdx mice. Post-HFD *mdx* blood glucose values did not worsen after a high fat diet, while *mdx/Sln*-null mice saw a significant worsening of their glucose intolerance. Future studies should examine whether utrophin (utr) expression is a key protein with respect to GLUT4 translocation. Animals for such a study may be difficult for a high fat feeding study, as *mdx* utr -/- mice have limited life spans and often die prematurely before reaching the 3-4-months age of mdx controls (McDonald et al., 2015). As such it proposed that a heterozygote model, *mdx* utr +/-, may provide an intermediate model. These *utr* heterozygous mdx mice display greater pathology than *mdx* mice but less than *mdx* utr -/- mice and their lifespans are almost normal in comparison to the short life spans of *mdx* utr -/- animals. Furthermore, these animals display haploinsufficient expression of utrophin and could provide further insight into the role of utrophin and glucose tolerance.

References

Anderson, J. E., Ovalle, W. K., & Bressler, B. H. (1987). Electron microscopic and autoradiographic characterization of hindlimb muscle regeneration in the mdx mouse. *Anatomical Record, 219*(3), 243-257.

Arita, Y., Kihara, S., Ouchi, N., Takahashi, M., Maeda, K., Miyagawa, J.,…Matsuzawa, Y. (1999). Paradoxical decrease of an adipose-specific protein, adiponectin, in obesity. *Biochemical and Biophysical Research Communications, 257*, 79-83.

Asahi, M., Sugita, Y., Kurzydlowski, K., De Leon, S., Tada, M., Toyoshima, C., & MacLennan, D. H. (2003). Sarcolipin regulates sarco(endo)plasmic reticulum Ca^{2+}-ATPase (SERCA) by binding to transmembrane helicies alone or in association with phospholamban. *Pnas, 100*(9), 5040-5045.

Bal, N. C., Maurya, S. L., Sopariwala, D. H., Sahoo, S. K., Gupta, S. C., Shaikh, S. A., & Periasamy, M. (2012). Sarcolipin is a newly identified regulator of muscle-based thermogenesis in mammals. *Nature Medicine, 18*(10), 1575-1579. doi:10.1038/nm.2897

Berchtold, M. W., et al. (2000). "Calcium Ion in Skeletal Muscle: Its Crucial Role for Muscle Function, Plasticity, and Disease." Physiological Reviews 80(3): 1215-1265.

Berman MC. Slippage and uncoupling in P-type cation pumps; implications for energy transduction mechanisms and regulation of metabolism. *Biochem. Biophys. Acta.* 1513: 95-121, 2001.

Blake, D. J., Weir, A., Newey, S. E., & Davies, K. E. (2002). Function and Genetics of Dystrophin and Dystrophin-Related Proteins in Muscle. *Physiological Reviews, 82*(2), 291-329.

Bombardier, E., Smith, I. C., Gamu, D., Fajardo, V. A., Vigna, C., Sayer, R. A., & Tupling, A. R. (2013). Sarcolipin trumps Beta-Adrenergic receptor signaling as the favored mechanism for muscle based diet-induced thermogenesis. *FASEB J, 2*(7), 3871-3878.

Bombardier, E., Smith, I. C., Vigna, C., Fajardo, V. A., & Tupling, A. R. (2013). Ablation of sarcolipin decreases the energy requirements for Ca2+ transport by sarco(endo)plasmic reticulum Ca2+-ATPases in resting skeletal muscle. *FEBS Letters, 587*, 1687-1692.

Bombarider, E. (2010). *The Role of Sarcolipin in Calcium Handling and Obesity.* (Unpublished Phd Thesis). University of Waterloo, Waterloo, Ontario, Canada.

Bonilla, E., Samitt, C. E., Miranda, A. F., Hays, A. P., Salviati, G., DiMauro, S., & Rowland, L. P. (1988). Duchenne Muscular Dystrophy: Defiency of Dystrophin at the Muscle Cell Surface. *Cell, 54*, 447-452.

Buettner, R., Schölmerich, J., & Bollheimer, L. C.High-fat diets: modeling the metabolic disorders of human obesity in rodents.. *Obesity, 15*(4), 798-808.

Bulfield, G., Siller, W. G., Wight, P. A. L., & Moore, K. J. (1984). X chromosome-linked muscular dystrophy (mdx) in the mouse. *81*. 1189-1192.

Cannon B, Nedergaard J. Brown adipose tissue: function and physiological significance. Physiol. Rev. 2004; 84(1):277Y359.

Cannon, B., & Nedergard, J. (2003). Brown Adipose Tissue: Function and physiological significance. *Physiological Reviews, 84*, 277-359.

Chu, V., Otero, J. M., Lopez, O., Sullivan, M. F., Morgan, J. P., Amende, I., & Hampton, T. G. (2002). Electrocardiographic findings in *mdx* mice: A cardiac phenotype of Duchenne muscular dystrophy. *Muscle and Nerve, 26*(4), 513-519.

Clausen, T. (1986). Regulation of active Na+-K+ transport in skeletal muscle. *Physiological Reviews,* (542), 580.

Collins, S., Martin, T. L., Surwit, R. S., & Robidoux, J. (2004). Genetic vulnerability to diet-induced obesity in the C57BL/6J mouse: physiological and molecular characteristics. *Physiology and Behavior, 81*(2), 243-248.

Connolly, A. M., Keeling, R. M., Mehta, S., Pestronk, A., & Sanes, J. R. (2001). Three mouse models of muscular dystrophy: the natural history of strength and fatigue in dystrophin-, dystrophin/utrophin-, and laminin alpha2-deficient mice. *Neuromuscular Disorders, 11*(8), 703-712.

Coulton, G. R., Curtin, N. A., Morgan, J. E., & Partridge, T. A. (1988). The mdx mouse skeletal muscle myopathy: II. Contractile properties. *Neuropathology and Applied Neurobiology, 14*(4), 299-314.

Culligan, K., Banville, N., Downling, P., & Ohlendieck, K. (2002). Drastic reduction of calsequestrin-like proteins and impaired calcium binding in dystrophic mdx muscle. *Journal of Applied Physiology, 92*, 435-445.

de Meis L. Role of the sarcoplasmic reticulum Ca2+-ATPase on heat production and thermogenesis. *Biosci. Rep.* 21: 113-137, 2001b.

de Meis L. Uncoupled ATPase activity and heat production by the sarcoplasmic reticulum Ca2+-ATPase: Regulation by ADP. *J. Biol. Chem.* 276: 25078-25087, 2001a.

deLany, J. P., & West, D. B. (2000). Changes in body composition with conjugated linoleic acid. *Journal of the American College of Nutrition, 19,* 487S-493S.

Dulhunty, A.F. (2006). Excitation-contraction coupling from the 1950s into the new millennium. *Clin ExPPharmacol Physiol.* 33: 763-772.

Dulloo, A. G., Gubler, M., Montani, J. P., Seydoux, J., & Solinas, G. (2004). Substrate cycling between de novo lipogenesis and lipid oxidation: a thermogenic mechanism against skeletal muscle lipotoxicity and glucolipotoxicity. *International Journal of Obesity, 28,* S29-S37.

Dupont-Versteegden, E. E., Baldwin, R. A., McCarter, R. J., & Vonlanthen, M. G. (1994). Does Muscular Dystrophy Affect Metabolic Rate? A Study in mdx mice. *Journal of Neurological Sciences, 121,* 203-207.

Dyck, D. J., Heigenhauser, G. J. F., & Bruce, C. R. (2006). The role of adipokines as regulators of skeletal muscle fatty acid metabolism and insulin sensitivity. *Acta Physiologica, 185,* 5-16.

Fajardo, V. A. (2015). *The Role of Phospholamban and Sarcolipin in Skeletal Muscle Disease.* (Unpublished Phd Thesis). University of Waterloo, Waterloo, Ontario, Canada.

Feldmann, H. M., Golozoubova, V., Cannon, B., & Nedergaard, J. (2009). UCP1 Ablation Induces Obesity and Abolishes Diet-Induced Thermogenesis in Mice Exempt from Thermal Stress by Living at Thermoneutrality. *Cell Metabolism, 9*(2), 203-209.

Feldmann, H.M., Golozoubova, V., Cannon, B., and Nedergaard, J. (2009). UCP-1 ablation induces obesity and abolishes diet-induced thermogenesis in mice exempt from thermal stress by living at thermoneutrality. *Cell Metab*. 9: 203-209.

Franco-Obregon Jr A, Lansman JB. Mechanosensitive ion channels in skeletal muscle from normal and dystrophic mice. *J. Physiol.* 1994; 481: 299–309.

Frank, K., Tilgmann, C., Shannon, T. R., Bers, D. M., & Kranias, E. G. (2000). Regulatory Role of Phospholamban in the Efficiency of Cardiac Sarcoplasmic Reticulum Ca2+ Transport. *Biochemical Journal, 39*, 14176-14182.

Gailly P. (2002) New aspects of calcium signaling in skeletal muscle cells: implications in Duchenne muscular dystrophy. *Biochim Biophys Acta* 1600(1-2):38-44.

Gamu, D. (2012). *Examination of Voluntary Wheel Running and Skeletal Muscle Metabolism in the Sarcolipin Knock-Out Mouse.* (Unpublished Master's Thesis). University of Waterloo, Waterloo, Ontario, Canada.

Garcia-Pelagio, K. P., Bloch, R. J., Ortega, A., & Gonzalez-Serratos, H. (2011). Biomechanics of the sarcolemma and costameres in single skeletal muscle fibers from normal and dystrophin-null mice. *Journal of Muscle Research and Cell Motility, 31*(0), 323-336. doi:10.1007/s10974-011-9238-9

Guilherme, A., Virbasius, J. V., Puri, V., & Czech, M. P. (2008). Adipocytes dysfunctions linking obesity to insulin resistance and type 2 diabetes. *Nature Reviews Molecular Cell Biology, 9*, 367-377.

Hoeks, J., Hesselink, M. K., & Schrauwen, P. (2006). Involvement of UCP3 in mild uncoupling and lipotoxicity. *Experimental Gerontology, 41*(7), 658-662.

Janovska, A., Hatzinikolas, G., Mano, M., & Wittert, G. A. (2010). The effect of dietary fat content on phospholipid fatty acid profile is muscle fibre-type dependent. *American Journal of Physiology, 298*(4), E779-E786.

Kashyap, S., Belfort, R., Gastaldelli, A., Pratipanawatr, T., Berria, R., Pratipanawatr, W., . . . Cusi, K. (2003). A sustained increase in plasma free fatty acids impairs insulin secretion in nondiabetic subjects genetically predisposed to develo*P*type 2 diabetes. *Diabetes, 52*(10), 2461-2474.

Kontani, Y., Wang, Y., Kimura, K., Inokuma, K. I., Saito, M., Suzuki-Miura, T., . . . Yamashita, H. (2005). UCP1 deficiency increases susceptibility to diet-induced obesity with age. *Aging Cell, 4*(3), 147-155.

Kuznetsov AV, Winkler K, Wiedemann FR, von Bossanyi P, Dietzmann K, Kunz WS. Impaired mitochondrial oxidative phosphorylation in skeletal muscle of the dystrophin-deficient *mdx* mouse. *Mol. Cell. Biochem.* 1998; 183: 87–96.

Li, B., Nolte, L. A., Ju, J., Han, D. H., Coleman, T., Holloszy, J. O., & Semenkovich, C. F. (2000). Skeletal muscle respiratory uncoupling prevents diet-induced obesity and insulin resistance in mice. *Nature Medicine, 6*(10), 1115-1120.

MacLean, P. S., Higgins, J. A., Johnson, G. C., Fleming-Elder, B. K., Donahoo, W. T., Melanson, E. L., & Hill, J. O. (2004). Enhanced metabolic efficiency contributes to weight regain after weight loss in obesity-prone rats. *American Journal of Physiology Regulatory Integrative and Comparative Physiology, 287*(6), 1306-1315.

MacLennan, D. H., Asahi, M., & Tupling, A. R. (2003). The regulation of SERCA-type pumps by phospholamban and sarcolipin. *Annals of the New York Academy of Sciences, 986*, 472-480.

Maickel, R. P., Matussek, N., Stern, D. N., & Brodie, B. B. (1967). The sympathetic nervous system as a homeostatic mechanism. I. Absolute need for sympathetic nervous function in body temperature maintenance of cold-exposed rats. *Journal of Phamacology and Experimental Therapeutics, 157*(1), 103-110.

Mall S, Broadbridge R, Harrison SL, Gore MG, Lee AG and East JM. The presence of sarcolipin results in increased heat production by Ca2+-ATPase. *J. Biol. Chem.* 281: 36597-36602, 2006.

Martonosi AN & Pikula S (2003) The network of calcium regulation in muscle. *Acta Biochim Pol* 50(1):1-30.

Maurya, S. K., Bal, N. C., Sopariwala, D. H., Pant, M., Rowland, L. A., Shaikh, S. A., & Periasamy, M. (2015). Sarcolipin Is a Key Determinant of the Basal Metabolic Rate, and Its

Overexpression Enhances Energy Expenditure and Resistance against Diet-induced Obesity. *The Journal of Biological Chemistry, 290*(17), January 25, 2017. doi:-10.1074/jbc.M115.636878

McDonald, A. A., Herbert, S. L., Kunz, M. D., RAlles, S. J., & McLoon, L. K. (2015). Disease course in *mdx:utrophin+/−* mice: comparison of three mouse models of Duchenne muscular dystrophy.*Physiological Reports, 3*(4) doi:10.14814/phy2.12391

McGreevy, J. W., Hakim, C. H., McIntosh, M. A., & Duan, D. (2015). Animal models of Duchenne muscular dstrophy: from basic mechanisms to gene therapy. *The Company of Biologists Disease Models and Mechanisms, 8*, 195-213.

Mokhtarian, A., Decrouy, A., Chinet, A., & Even, P. C. (1996). Components of energy expenditure in the mdx mouse model of Duchene muscular dystrophy. *European Journal of Physiology, 431*, 527-532.

Percival, J. M., Siegel, M. P., Knowels, G., & Marcinek, D. J. (2013). Defects in mitochondrial localization and ATP synthesis in the *mdx* mouse model of Duchenne muscular dystrophy are not alleviated by PDE5 inhibition. *Human Molecular Genetics, 22*(1), 153-167.

Pertille, A., Tonizza de Carvallo, C. L., Matsumura, C. Y., Neto, H. S., & Marques, M. J. (2010). Calcium-binding proteins in skeletal muscles of the mdx mice: potential role in the pathogenesis of Duchenne muscular dystrophy. *International Journal of Experimental Pathology, 91*, 63-71.

Petrof, B. J., Shrager, J. B., Stedman, H. H., Kelly, A. M., & Sweeney, H. L. (1993). Dystrophin protects the sarcolemma from stresses during muscle contraction. *Proceedings of the National Academy of Sciences of the United States of America, 90*, 3710-3714.

Radley, H. G., De Luca, A., Lynch, G. S., & Grounds, M. D. (2007). Duchenne muscular dystrophy: Focus on pharmaceutical and nutritional interventions. *The International Journal of Biochemistry & Cell Biology, 39*, 469-477.

Radley-Crabb, H. G., Fiorotto, M. L., & Grounds, M. D. (2011). The different impact of a high fat diet on dystrophic mdx and control C57Bl/10 mice. *PLOS Currents Muscular Dystrophy*, (1) doi:10.1371/currents.RRN1276.

Radley-Crabb, H. G., Marini, J. C., Sosa, H. A., Castillo, L. I., Grounds, M. D., & Fiorotto, M. L. (2014). Dystropathology Increases Energy Expenditure and Protein Turnover in the Mdx Mouse Model of Duchenne Muscular Dystrophy. *PLOS One, 9*(2), 1-13. doi:10.1371/journal.pone.0089277

Reis M, Farage M and de Meis L. Thermogenesis and energy expenditure: control of heat production by the Ca2+-ATPase of fast and slow muscle. *Mol. Mem. Biol.* 19: 301-310, 2002.

Roden, M., Price, T. B., Perseghin, G., Petersen, K. F., Rothman, D. L., Cline, G. W., & Shulman, G. I. (1996). Mechanism of free fatty acid-induced insulin resistance in humans. *Journal of Clinical Investigation, 97*, 2859-2865.

Rolfe, D. F., & Brown, G. C. (1997). Cellular energy utilization and molecular origin of standard metabolic rate in mammals. *Physiological Reviews, 77*, 731-758.

Rowland, L. A., Maurya, S. K., Bal, N. C., Kozak, L., & Periasamy, M. (2016). Sarcolipin and uncoupling protein 1 play distinct roles in diet-induced thermogenesis and do not compensate for one another..*Obesity, 24*(7), 1430-1433.

Sarraf, P., Frederich, R. C., Turner, E. M., Ma, G., Jaskowiak, N. T., Rivet, D. J., . . . Alexander, H. R. (1997). Multiple cytokines and acute inflammation raise mouse leptin levels: potential role in inflammatory anorexia. *The Journal of Experimental Medicine, 185*(1), 171-175.

Schiaffino S & Reggiani C (2011) Fiber types in mammalian skeletal muscles. *Physiol Rev* 91(4):1447-1531.

Schneider, J. S., SHanmugam, M., Gonzalez, J. S., Lopez, H., Gordan, R., Fraidenraich, D., & Babu, G. J. (2013). Increased sarcolipin expression and decreased sarco(endo)plasmic reticulum Ca2+ uptake in skeletal muscles of mouse models of Duchenne muscular dystrophy. *Journal of Muscle Research and Cell Motility,34*, 349-356. doi:10.1007/s10974-013-9350-0

Schrauwen, P., Hoppeler, H., Billeter, R., Bakker, A., & Pendergast, D. (2001). Fibre type dependent upregulation of human skeletal muscle UCP2 and UCP3 mRNA expression by high fat diet. *International Journal of Obesity and Related Metabolic Disorders, 25*(4), 449-456.

Shiota, M., & Masumi, S. (1988). Effect of norepinephrine on consumption of oxygen in perfused skeletal muscle from cold exposed rats. *American Journal of Physiology, 254*, E482-E489.

Sicinski, P., Geng, Y., Ryder-Cook, A. S., Barnard, E. A., Darlison, M. G., & Barnard, P. J. (1989). The Molecular Basis of Muscular Dystrophy in the mdx Mouse: A Point Mutation. *Science, 244*, 1578-1579.

Smith, I. C., Bombardier, E., Vigna, C., & Tupling, A. R. (2013). AT*P*Consumption by Sarcoplasmic Reticulum Ca^{2+} Pumps Accounts for 40-50% of Resting Metabolic Rate in Mouse Fast and Slow Twitch Skeletal Muscle. *PLOS One, 8*(7), 1-11.

Smith, W. S., Broadbridge, R., East, J. M., & Lee, A. G. (2002). Sarcolipin uncouples the hydrolysis of AT*P*from accumulation of Ca^{2+} by the Ca^{2+}-ATPase of the skeletal-muscle sarcoplasmic reticulum. *Biochemical Journal, 361*, 277-286.

Son, C., Hosoda, K., Ishihara, K., Bevilaqua, L., Masuzaki, H., Fushiki, T., Harper, M.E., and Nakao, K. (2004). Reduction in diet-induced obesity in transgenic mice overexpressing uncoupling protein 3 in skeletal muscle. *Diabetologia*. 47: 47-54.

Spencer MJ, Croall DE, Tidball JG. Calpains are activated in necrotic fibers from *mdx* dystrophic mice. *J. Biol. Chem.* 1995; 270: 10 909–914

Stammers, A. N., et al. (2015). "The regulation of sarco(endo)plasmic reticulum calcium-ATPases (SERCA)." Canadian Journal of Physiology and Pharmacology 93(10): 843-854.

Stapleton, D. I., Lau, X., Flores, M., Trieu, J., Gehrig, S. M., Chee, A., . . . Koopman, R. (2014). Dysfunctional muscle and liver glycogen metabolism in mdx dystrophic mice. *PLOS One, 9*(3) doi:10.1371/journal.pone.0091514

Tidball, J. G. (2005). Inflammatory processes in muscle injury and repair. *American Journal of Physiology Regulatory Integrative and Comparative Physiology, 288*(2), 345-353.

Toyoshima C & Inesi G (2004) Structural basis of ion pumping by Ca2+-ATPase of the sarcoplasmic reticulum. *Annu Rev Biochem* 73:269-292.

Toyoshima C, Nakasako M, Nomura H, & Ogawa H (2000) Crystal structure of the calcium pum*P*of sarcoplasmic reticulum at 2.6 A resolution. *Nature* 405(6787):647-655.

Toyoshima, C. (2007). Ion Pumping by Calcium ATPase of sarcoplasmic reticulum. *Advances in Experimental Medicine and Biology, 592*, 295-303.

Tupling, A. R., Bombardier, E., Gupta, S. C., Hussain, D., Vigna, C., Bloemberg, D., & Gramolini, A. O. (2011). Enhanced Ca^{2+} transport and muscle relaxation in skeletal muscle from sarcolipin-null mice. *American Journal of Physiology Cell Physiology, 301*, 841-849.

Turner PR, Fong PY, Denetclaw WF, Steinhardt RA. Increased calcium influx in dystrophic muscle. *J. Cell Biol.* 1991; 115: 1701–12.

Turner, P. R., Westwood, T., Regen, C. M., & Steinhardt, R. A. (1988). Increased protein degradation results from elevated free calcium levels found in muscle from mdx mice. *Nature, 335*, 735-738.

Vangheluwe P, Schuermans M, Zador E, Waelkens E and Raeymaekers L.(2005a) Sarcolipin and phospholamban mRNA and protein expression in cardiac and skeletal muscle of different species. *Biochem. J.* 389: 151-159.

Vaugheluwe, P., Raeymaekers, L., Dode, L., & Wuytack, F. (2005b). Modulating sarco(endo)plasmic reticulum Ca2+ ATPase 2 (SERCA2) activity: cell biological implications. *Cell Calcium, 38*, 291-302.

Vidal-Puig, A., Solanes, G., Grujic, D., Flier, J.S., and Lowell, B.B. (1997). UCP3: An uncoupling protein homologue expressed preferentially and abundantly in skeletal muscle and brown adipose tissue. *Biochem Biophys Res Commun.* 235: 79-82.

Vidal-Puig, A.J., Grujic, D., Zhang, C.Y., Hagan, T., Boss, O., Ido, Y., Szczepanik, A., Wade, J., Mootha, V., Cortright, C., Muoio, D.M., and Lowell, B.B. (2000). Energy metabolism in uncoupling protein 3 gene knockout mice. *J Biol Chem*. 275: 16258–16266.

Voit A., Patel V., Pachon R., Shah V., Bakhutma M., Kohlbrenner E., McArdle J.J., Dell'Italia L.J., Mendell J.R., Xie LH, Hajjar R.J., Duan D., Fraidenraich D., Babu G.J. (2017). Reducing sarcolipin expression mitigates Duchenne muscular dystrophy and associated cardiomyopathy in mice. *Nature Communications, 8*(1). 1068.

West, D. B., & York, B. (1998). Dietary fat, genetic predisposition, and obesity: lessons from animal models. *American Journal of Clinical Nutrition, 67*(3 suppl), 505S-512S.

Whitehead, N. P., et al. (2006). "Muscle Damage in *mdx* (Dystrophic) mice: Role of Calcium and Reactive Oxygen Species." Clinical and Experimental Pharmacology and Physiology 33(7): 657-662.

Willmann, R., Possekel, S., Dubach-Powell, J., & Meier, M. (19). Mammalian animal models for Duchenne muscular dystrophy. *2009.* 241-249.

Woods, C. E., Novo, D., DiFranco, M., & Vergara, J. L. (2004). The action potential-evoked sarcoplasmic reticulum calcium release is impaired in mdx mouse muscle fibres. *Journal of Physiology, 557*(1), 59-75.

Zanardi, M. C., Tagliabue, A., Orcesi, S., Berardinelli, A., Uggetti, C., & Pichiecchio, A. (2003). Body composition and energy expenditure in Duchene muscular dystrophy. *European Journal of Clinical Nutrition, 57*, 273-278.

Appendix A: Supplementary Results

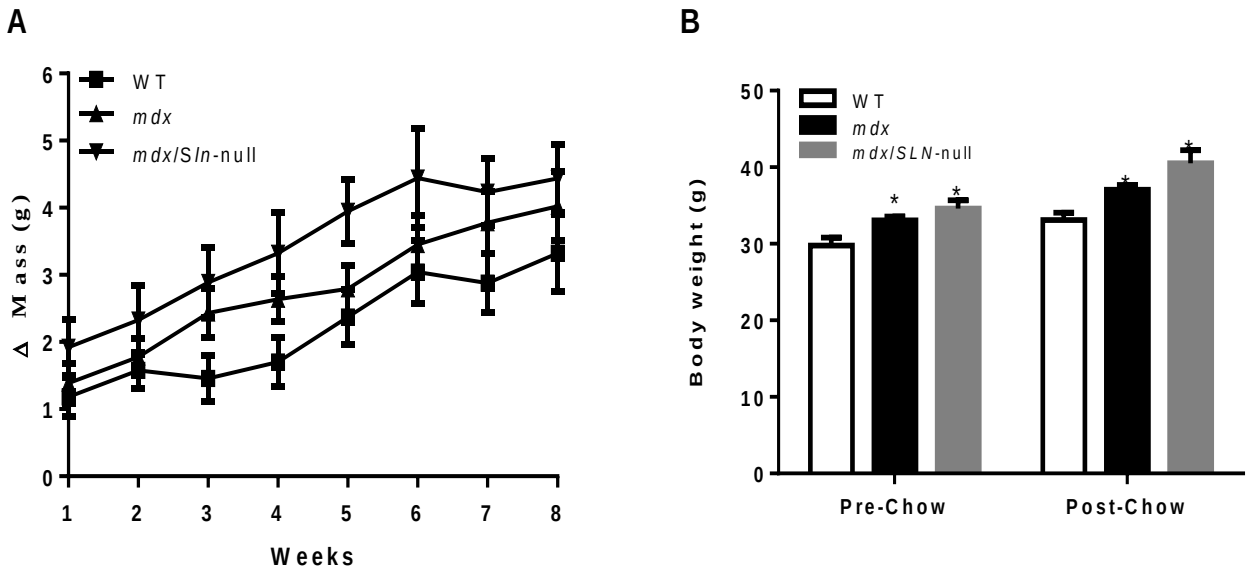

Figure A1. No differences in the change in body mass across all three genotypes, with mdx/ mdx/Sln-null mice having greater bodyweight pre- and post-Chow diet. A) Change in body mass of wild-type (WT), *mdx*, and *mdx/Sln*-null mice during 8 weeks of a Chow diet. B) Pre- and Post-Chow bodyweights of WT, *mdx*, and *mdx/Sln*-null mice. Values are mean ± S.E. * Significantly different than corresponding *mdx* and *mdx*/*Sln*-null ($P < 0.05$). (WT: n = 11, *m*dx: n = 13, *mdx*/*Sln*-null; n = 8)

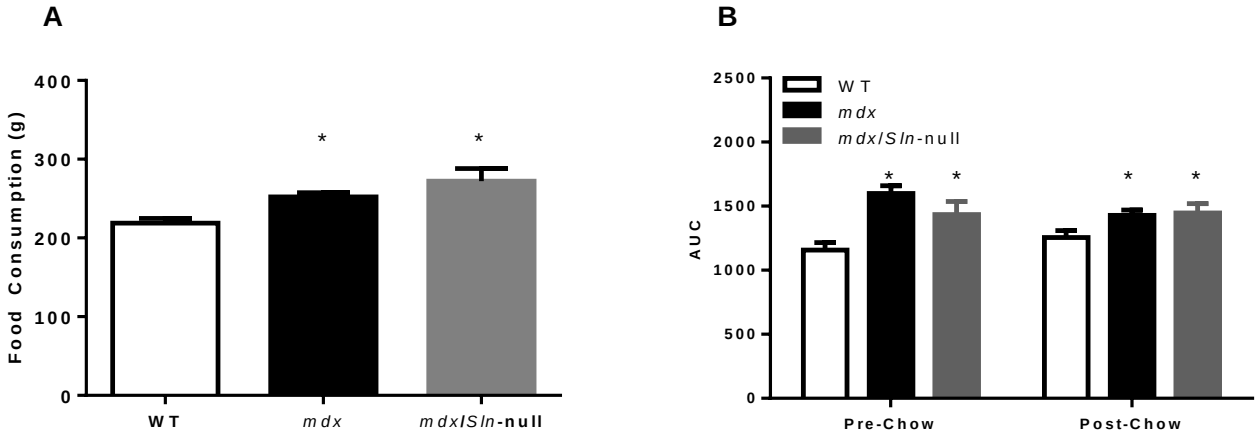

Figure A2. A) Total Food Consumption across 8 weeks of chow diet for wild-type (WT), *mdx*, and *mdx/Sln*-null mice. B) Glucose AUC *Significantly different from WT mice. Values are mean ± S.E. * Significantly different than *mdx* ($P < 0.05$). WT: n = 11, *m*dx: n = 13, *mdx*/*Sln*-null; n = 8)

Table A1. CLAMS Measurements of Wild type (WT), *mdx*, and *mdx/Sln*-null mice Pre and Post Chow

	Pre			Post		
	WT	*mdx*	*mdx/Sln*-null	WT	*mdx*	*mdx/Sln*-null
Body Weight (g)	29.7 ± 0.91	33.4 ± 0.52#	34.6 ± 1.1#	33.6 ± 0.97	37.0 ± 0.64*#	40.5 ± 1.54*#
Waking VO_2 (ml O_2/kg/hr)	3562 ± 41	3498 ± 65#	3224 ± 67#$	3192 ± 76*	3268 ± 68*#	2952 ± 63*#$
Sleeping VO_2 (ml O_2/kg/hr)	2793 ± 68	2775 ± 80#	2440 ± 52#$	2529± 62*	2547 ± 83*	2260 ± 77*#$
Total Daily VO_2 (ml O_2/kg/hr)	3319 ± 32	3291 ± 73#	2899 ± 66#$	2963 ± 56*	3069 ± 46*#	2705 ± 63*#$
Food Intake (g)	4.11 ± 0.18	4.26 ± 0.17	4.16 ± 0.22	4.17 ± 0.16	3.94 ± 0.09	3.83 ± 0.26
Metabolizable Energy (kcal)	11.51 ± 0.74	12.53 ± 0.49	12.53 ± 0.69	12.51 ± 0.48	11.55 ± 0.52	11.56 ± 0.49
Total Activity	9986 ± 550	7709 ± 356#	7176 ± 401#	10146 ± 671	7401 ± 266#	7383 ± 435#
Dual Beam Activity	3351 ± 405	2707 ± 124#	2429 ± 187#	3125 ± 359	2505 ± 136#	2341 ± 109#

Waking VO_2 (ml O_2/hr)	106 ± 3.0	117 ± 2.1#	118 ± 4.7#	107 ± 3.2	121 ± 2.6#	119 ± 3.6#
Sleeping VO_2 (ml O_2/hr)	83 ± 3.0	92 ± 2.4#	89 ± 4.4#	85 ± 2.2	94.2 ± 2.6#	92 ± 3.9#
Daily VO_2 (ml O_2/hr)	98 ± 2.5	110 ± 3.0#	106 ± 4.2#	100 ± 3.3	114 ± 2.4#	110 ± 3.5#
Awake RER	0.927 ± 0.009	0.926 ± 0.007	0.908 ± 0.006	0.934 ± 0.01	0.941 ± 0.005	0.908 ± 0.01
Sleep RER	0.899 ± 0.012	0.890 ± 0.007	0.888 ± 0.009	0.893 ± 0.011	0.899 ± 0.008	0.875 ± 0.014
Total RER	0.912 ± 0.01	0.904 ± 0.006	0.893 ± 0.005	0.923 ± 0.007	0.910 ± 0.007	0.901 ± 0.006

Main effect of age (Pre < Post) for Body Weight (P<.0001). Main effect of genotype (*mdx* > WT & *mdx/Sln*-null) for relative total daily VO_2 (P < 0.05), relative waking VO_2 (P < 0.05), and relative sleeping VO_2 (P < 0.05). Main effect of genotype (*mdx* & *mdx/Sln*-null > WT) for absolute total daily VO_2 (P < 0.05), absolute waking VO_2 (P < 0.05), and absolute sleeping VO_2 (P < 0.05). *Significantly different from Pre (P<0.05). #Significantly different from WT. $ Significantly different than *mdx*. VO_2, oxygen consumption, RER, respiratory exchange ratio. Values are Mean ± SEM (WT: n = 11, *m*dx: n = 13, *mdx*/*Sln*-null; n = 8)

Appendix B: Product Sheet of Mice Chow Diet

8640

ENVIGO

Teklad 22/5 Rodent Diet

Product Description- 8640 is a fixed formula, non-autoclavable diet manufactured with high quality ingredients and designed to support growth and reproduction of rodents. Typical isoflavone concentrations (daidzein + genistein aglycone equivalents) range from 350 to 650 mg/kg.

Ingredients (in descending order of inclusion)- Dehulled soybean meal, ground corn, wheat middlings, flaked corn, fish meal, cane molasses, soybean oil, ground wheat, dried whey, dicalcium phosphate, calcium carbonate, brewers dried yeast, iodized salt, choline chloride, kaolin, magnesium oxide, ferrous sulfate, vitamin E acetate, menadione sodium bisulfite complex (source of vitamin K activity), manganous oxide, copper sulfate, zinc oxide, niacin, thiamin mononitrate, vitamin A acetate, vitamin D_3 supplement, calcium pantothenate, pyridoxine hydrochloride, riboflavin, vitamin B_{12} supplement, folic acid, calcium iodate, biotin, cobalt carbonate.

Standard Product Form: *Pellet*

Macronutrients		
Crude Protein	%	22.0
Fat (ether extract) [a]	%	5.5
Carbohydrate (available) [b]	%	40.6
Crude Fiber	%	3.9
Neutral Detergent Fiber [c]	%	12.8
Ash	%	8.1
Energy Density [d]	kcal/g (kJ/g)	3.0 (12.6)
Calories from Protein	%	29
Calories from Fat	%	17
Calories from Carbohydrate	%	54
Minerals		
Calcium	%	1.1
Phosphorus	%	0.9
Non-Phytate Phosphorus	%	0.6
Sodium	%	0.4
Potassium	%	1.0
Chloride	%	0.7
Magnesium	%	0.2
Zinc	mg/kg	77
Manganese	mg/kg	102
Copper	mg/kg	24
Iodine	mg/kg	3
Iron	mg/kg	280
Selenium	mg/kg	0.27
Amino Acids		
Aspartic Acid	%	2.1
Glutamic Acid	%	3.6
Alanine	%	1.2
Glycine	%	1.1
Threonine	%	0.9
Proline	%	1.4
Serine	%	1.4
Leucine	%	1.7
Isoleucine	%	1.0
Valine	%	1.1
Phenylalanine	%	1.1
Tyrosine	%	0.9
Methionine	%	0.4
Cystine	%	0.3
Lysine	%	1.2
Histidine	%	0.6
Arginine	%	1.4
Tryptophan	%	0.3

Vitamins		
Vitamin A [*,f]	IU/g	15.8
Vitamin D_3 [*,g]	IU/g	3.0
Vitamin E	IU/kg	150
Vitamin K_3 (menadione)	mg/kg	50
Vitamin B_1 (thiamin)	mg/kg	32
Vitamin B_2 (riboflavin)	mg/kg	9
Niacin (nicotinic acid)	mg/kg	66
Vitamin B_6 (pyridoxine)	mg/kg	14
Pantothenic Acid	mg/kg	23
Vitamin B_{12} (cyanocobalamin)	mg/kg	0.06
Biotin	mg/kg	0.41
Folate	mg/kg	3
Choline	mg/kg	2380
Fatty Acids		
C16:0 Palmitic	%	0.7
C18:0 Stearic	%	0.2
C18:1ω9 Oleic	%	1.1
C18:2ω6 Linoleic	%	2.5
C18:3ω3 Linolenic	%	0.2
Total Saturated	%	0.9
Total Monounsaturated	%	1.2
Total Polyunsaturated	%	2.7
Other		
Cholesterol	mg/kg	30

[a] Ether extract is used to measure fat in pelleted diets, while an acid hydrolysis method is required to recover fat in extruded diets. Compared to ether extract, the fat value for acid hydrolysis will be approximately 1% point higher.

[b] Carbohydrate (available) is calculated by subtracting neutral detergent fiber from total carbohydrates.

[c] Neutral detergent fiber is an estimate of insoluble fiber, including cellulose, hemicellulose, and lignin. Crude fiber methodology underestimates total fiber.

[d] Energy density is a calculated estimate of *metabolizable energy* based on the Atwater factors assigning 4 kcal/g to protein, 9 kcal/g to fat, and 4 kcal/g to available carbohydrate.

[*] Indicates added amount but does not account for contribution from other ingredients.

[f] 1 IU vitamin A = 0.3 µg retinol

[g] 1 IU vitamin D = 25 ng cholecalciferol

For nutrients not listed, insufficient data is available to quantify.

Nutrient data represent the best information available, calculated from published values and direct analytical testing of raw materials and finished product. Nutrient values may vary due to the natural variations in the ingredients, analysis, and effects of processing.

Teklad Diets are designed and manufactured for research purposes only.

© 2015 Envigo

DH15

Teklad Diets + Madison WI + envigo.com + tekladinfo@envigo.com + (800) 483-5523

Appendix C: Product Sheet of High Fat Diet

ENVIGO

Research Models and Services

Teklad Custom Diets

TD.88137 Adjusted calories diet (42% from fat)

A staple of atherosclerosis research

More than 25 years ago, our nutritionists collaborated with researchers at Rockefeller University to develop a diet with features of a 'Western Diet' to characterize and enhance atherosclerosis development in their newly generated *Apoe* deficient mouse model. With over 200 unique users worldwide, TD.88137 continues to be fed to genetically modified cardiovascular models to accelerate and enhance hypercholesterolemia and plaque formation.

Formula	g/Kg
Casein	195.0
DL-Methionine	3.0
Sucrose	341.46
Corn Starch	150.0
Andydrous Milkfat	210.0
Cholesterol	1.5
Cellulose	50.0
Mineral Mix, AIN-76 (170915)	35.0
Calcium Carbonate	4.0
Vitamin Mix, Teklad (40060)	10.0
Ethoxyquin	0.04

Selected nutrient information[1]

	% By weight	% kcal from
Protein	17.3	15.2
Carbohydrate	48.5	42.7
Fat	21.2	42.0
kcal/g	4.5	
Cholesterol[2]	0.2%	

[1] Values are calculated from ingredient analysis or manufacturer data.
[2] 0.15% added, 0.05% from fat source.

Teklad diets are designed and manufactured for research purposes only.

Critical dietary features of TD.88137 related to atherosclerosis development include:

+ Cholesterol (0.2% total cholesterol)
+ Total fat (21% by weight; 42% kcal from fat)
+ High in saturated fatty acids (>60% of total fatty acids)
+ High sucrose (34% by weight)

Typical fatty acid profile of TD.88137

Typical fatty acid analysis, % of diet[1]	Mean	SD
Total	20.7	1.5
Saturated fat	12.8	0.8
Monounsaturated fat	5.6	0.5
Polyunsaturated fat	1.0	0.2
Unknown[2]	1.3	0.3

Typical fatty acid profile, % of total fatty acids[1]	Mean	SD
Saturated fat	61.8	2.0
Monounsaturated fat	27.3	2.1
Polyunsaturated fat	4.7	0.8
4:0	2.1	1.1
6:0	1.5	0.7
8:0	1.1	0.3
10:0	2.6	0.5
12:0	3.3	0.5
14:0	10.6	0.9
16:0	28.9	1.3
16:1	1.5	0.2
18:0	12.5	0.8
18:1 (Oleic)	20.9	2.6
18:1 Isomers[3]	4.0	1.2
18:2 (Linoleic)	2.3	1.0
18:2 Isomers[4]	1.3	0.5
18:3 (Linolenic)	0.7	0.2

[1] n = 21, analysis conducted by two independent laboratories.
[2] Unidentified fatty acids and those contributing on average less than 0.5% of total fatty acids.
[3] Includes trans isomers elaidic and vaccenic acid and unidentified cis isomers.
[4] Includes trans isomers.

North America 800.483.5523 EU and Asia envigo.com/contactus teklad@envigo.com envigo.com

Appendix C: Product Sheet of High Fat Diet

Key points from the literature

TD.88137 has been used to accelerate atherosclerosis development in *Apoe* and *Ldlr* deficient models:

+ In *Apoe* deficient mice, plasma cholesterol triples to >1500 mg/dL within three weeks (1, 2). Foam cell and lesion development occurs within 6-10 weeks (2-4). Fibrous plaque formation is observed at 15 weeks with the development of fibrous caps after 20 weeks (2).
+ *Ldlr* deficient mice fed for two weeks increase plasma cholesterol to >800 mg/dL and triglyceride to >300 mg/dL (5). After six weeks of feeding, hyperglycemia, hyperinsulinemia and dyslipidemia develop with small foam cell lesions in the aortic arch (6, 7).

For further information about TD.88137, or if you are interested in learning more about other atherogenic or high fat diets contact us at: **askanutritionist@envigo.com**

With over 420 citations, uses of TD.88137 continue to evolve and include atherosclerosis, obesity, non-alcoholic steatohepatitis (NASH), osteoporosis, hypertension and metabolic syndrome. Contact us for a more extensive reference list.

References

1. **Plump, A.S., et al.,** Severe hypercholesterolemia and atherosclerosis in apolipoprotein E-deficient mice created by homologous recombination in ES cells. *Cell, 1992. 71(2):* p. 343-53.
2. **Nakashima, Y., et al.,** Apoe-deficient mice develop lesions of all phases of atherosclerosis throughout the arterial tree. *Arterioscler Thromb, 1994. 14(1):* p. 133-40.
3. **Febbraio, M., et al.,** Targeted disruption of the class B scavenger receptor CD36 protects against atherosclerotic lesion development in mice. *J Clin Invest, 2000. 105(8):* p. 1049-56.
4. **Nakashima, Y., et al.,** Upregulation of VCAM-1 and ICAM-1 at atherosclerosis-prone sites on the endothelium in the Apoe-deficient mouse. *Arterioscler Thromb Vasc Biol, 1998. 18(5):* p. 842-51.
5. **Towler, D.A., et al.,** Diet-induced diabetes activates an osteogenic gene regulatory program in the aortas of low density lipoprotein receptor-deficient mice. *J Biol Chem, 1998. 273(44):* p. 30427-34.
6. **Tsuchiya, K., et al.,** FoxOs integrate pleiotropic actions of insulin in vascular endothelium to protect mice from atherosclerosis. *Cell Metab, 2012. 15(3):* p. 372-81.
7. **Huszar, D., et al.,** Increased LDL cholesterol and atherosclerosis in LDL receptor-deficient mice with attenuated expression of scavenger receptor B1. *Arterioscler Thromb Vasc Biol, 2000. 20(4):* p. 1068-73.
8. **Yang, B., et al.,** Changes of skeletal muscle adiponectin content in diet-induced insulin resistant rats. *Biochem Biophys Res Commun, 2006. 341(1):* p. 209-17.
9. **Schafer, K., et al.,** Leptin promotes vascular remodelling and neointimal growth in mice. *Arterioscler Thromb Vasc Biol, 2004. 24(1):* p. 112-7.
10. **Lijnen, H.R., et al.,** Nutritionally induced obesity is attenuated in transgenic mice overexpressing plasminogen activator inhibitor-1. *Arterioscler Thromb Vasc Biol, 2003. 23(1):* p. 78-84.
11. **Maquoi, E., et al.,** Modulation of adipose tissue expression of murine matrix metalloproteinases and their tissue inhibitors with obesity. *Diabetes, 2002. 51(4):* p. 1093-101.
12. **VanSaun MN, et al. 2009.** High fat diet induced hepatic steatosis establishes a permissive microenvironment for colorectal metastases and promotes primary dysplasia in a murine model. *Am J Pathol 175:355-64.*
13. **Dixon LJ, et al. 2013.** Caspase-1 as a central regulator of high fat diet-induced non-alcoholic steatohepatitis. *PLoS One 8e56100.*

Control diet options for TD.88137

Natural ingredient diets

+ Also referred to as standard diets or chow
+ Diets differ in the source and level of nutrients as well as the presence of non-nutritive factors (such as phytates or phytoestrogens) compared to TD.88137
+ Limits inferences to differences in dietary pattern versus a specific dietary component

Ingredient matched, low fat diets

+ Controls for the type of ingredients, non-nutritive components and the source and level of specific nutrients
+ Suggested ingredient matched, low fat dietary controls for TD.88137 listed below; data sheets can be found on our website at envigo.com

Suggested ingredient matched, low fat controls

Diet	kcal/g	Fat, % by weight	% kcal from fat	Fat sources, % by weight	Sucrose, % by weight
TD.05230	3.7	5.2	12.6	3.7% milk fat, 1.3% soybean oil	34.1
TD.08485	3.6	5.2	13.0	3.7% milk fat, 1.3% soybean oil	12.0

Additional controls are available. Contact a nutritionist at askanutritionist@envigo.com.

Key planning information:

- Store diet refrigerated and plan to use within six months. Diet should be replaced at minimum once per week when fed on cage tops.
- Diets available as a soft ½" pellet or as a crumbly powder.
- Three kg minimum order quantity. For planning purposes, estimates for diet uses (including feed intake and diet waste) are 5 g of diet per mouse and 30 g of diet per rat per day.
- Two-day lead time for orders less than 10 kg. Two-week lead time for larger quantity orders.
- Lead time for irradiation adds two weeks for any quantity of diet and must be requested at the time you place your order. Changes in texture and browning may occur with irradiation.
- Shipping can affect pellet quality. Vacuum packaging can offer protection of the pellets during shipping. Two-day shipping is recommended during warmer months.
- Contact us to place an order, obtain pricing or check your order status.

Contact us

North America 800.483.5523 EU and Asia envigo.com/contactus teklad@envigo.com

Envigo RMS Division, 8520 Allison Pointe Blvd., Suite 400, Indianapolis, IN 46250, United States

© 2016 Envigo.

envigo.com

RMS-0716-US-02-PS-148